

UNCLASSIFIED

AD NUMBER

AD466165

LIMITATION CHANGES

TO:

Approved for public release; distribution is unlimited.

FROM:

**Distribution authorized to U.S. Gov't. agencies and their contractors;
Administrative/Operational Use; JUL 1965. Other requests shall be referred to Air Force Arnold Engineering Development Center, Arnold AFB, TN.**

AUTHORITY

aedc ltr, 12 nov 1965

THIS PAGE IS UNCLASSIFIED



**EXPERIMENTAL HEAT TRANSFER TO HEMISPHERES IN
NONEQUILIBRIUM DISSOCIATED HYPERSONIC FLOW WITH
SURFACE CATALYSIS AND SECOND-ORDER EFFECTS**

William H. Carden
ARO, Inc.

July 1965

PROPERTY OF U. S. AIR FORCE
AEDC LIBRARY
AF 40(600)1200

**VON KÁRMÁN GAS DYNAMICS FACILITY
ARNOLD ENGINEERING DEVELOPMENT CENTER
AIR FORCE SYSTEMS COMMAND
ARNOLD AIR FORCE STATION, TENNESSEE**

NOTICES

When U. S. Government drawings specifications, or other data are used for any purpose other than a definitely related Government procurement operation, the Government thereby incurs no responsibility nor any obligation whatsoever, and the fact that the Government may have formulated, furnished, or in any way supplied the said drawings, specifications, or other data, is not to be regarded by implication or otherwise, or in any manner licensing the holder or any other person or corporation, or conveying any rights or permission to manufacture, use, or sell any patented invention that may in any way be related thereto.

Qualified users may obtain copies of this report from the Defense Documentation Center.

References to named commercial products in this report are not to be considered in any sense as an endorsement of the product by the United States Air Force or the Government.

EXPERIMENTAL HEAT TRANSFER TO HEMISPHERES IN
NONEQUILIBRIUM DISSOCIATED HYPERSONIC FLOW WITH
. SURFACE CATALYSIS AND SECOND-ORDER EFFECTS

William H. Carden
ARO, Inc.

FOREWORD

The research reported herein was sponsored by the Arnold Engineering Development Center (AEDC), Air Force Systems Command (AFSC), under Program Element 62405334/8950.

The results of the research presented were obtained by ARO, Inc. (a subsidiary of Sverdrup and Parcel, Inc.), contract operator of AEDC, AFSC, Arnold Air Force Station, Tennessee, under Contract AF 40(600)-1000. The experimental work was conducted during August and September, 1964 under ARO Project Nos. VL2407 and VL2517, and the report was submitted by the author on June 1, 1965.

The author is indebted to his colleagues for their assistance during this investigation. John T. Miller designed the heat transfer probes and assisted in the experimental work. His earlier work provided the basis for many of the experimental techniques used. The silicon monoxide coatings for the heat transfer probes were provided by R. P. Young. Max Kinslow provided computer solutions for the nonequilibrium nozzle expansion. The author is particularly indebted to J. Leith Potter for suggesting the problem and for his patient display of confidence during the work.

Comments were received from several persons outside the author's organization. In particular, the comments of Dr. R. S. Hickman and Dr. H. K. Cheng were most helpful. Finally, the author is indebted to Dr. Daniel E. Rosner, whose brief presentation at the 1963 AIAA-ASME Hypersonic Ramjet Conference first aroused the author's interest in the subjects considered in this report.

This technical report has been reviewed and is approved.

Larry R. Walter
1st Lt, USAF
Gas Dynamics Division
DCS/Research

Donald R. Eastman, Jr.
DCS/Research

ABSTRACT

An experimental investigation of heat transfer to hemispheres with both catalytic and noncatalytic surfaces in nonequilibrium dissociated hypersonic nitrogen flow has been conducted. The wind tunnel flow conditions provided low Reynolds numbers, allowing the assumption of completely frozen shock and boundary layers while introducing the influences of second-order boundary layer effects such as vorticity interaction. The results for copper surfaces, when correlated using the stagnation point heat transfer equation of Rosner together with Lees' heat transfer distribution, are in good agreement with the second-order theory of Cheng under the assumption of complete surface recombination of atoms. Reductions in heat transfer rate up to 80 percent were obtained with the use of noncatalytic coatings applied to the probes.

CONTENTS

	<u>Page</u>
ABSTRACT	iii
NOMENCLATURE	vi
I. INTRODUCTION	1
II. FLOW CONDITIONS	
2.1 The Wind Tunnel	4
2.2 Flow Diagnosis	5
2.3 Boundary Layer Conditions	10
III. HEAT TRANSFER PROBES	12
IV. EXPERIMENTAL RESULTS	
4.1 Treatment of Data	13
4.2 Surface Behavior	15
4.3 Effect of Finite Catalyticity	17
4.4 Results for Copper Surfaces	18
4.5 Results for Coated Surfaces	19
4.6 Comparison with Previous Measurements	20
V. CONCLUSIONS	21
REFERENCES	22

ILLUSTRATIONS

Figure

1. Photograph of Gas Dynamic Wind Tunnel, Hypersonic (L) from the Operator's Side	29
2. Total-Enthalpy and Mass-Flow Probe Installed in Tunnel	30
3. Dissociation Fraction Measured by Nitric Oxide Titration	31
4. Water-Cooled Heat Transfer Probe	32
5. Effect of Finite Surface Catalytic Properties	33
6. Heat Transfer to Copper Hemispheres for $\phi = 1$	34
7. Heat Transfer to Copper Hemispheres for $\gamma_w = 1$	35
8. Heat Transfer to Hemispheres with Coated Surfaces	36
9. Some Previous Stagnation Heat Transfer Measurements at Low Reynolds Numbers	37

TABLE

	<u>Page</u>
I. Tunnel Flow Conditions	38

NOMENCLATURE

a	Hemisphere radius
c_p	Specific heat
D	Diffusion coefficient
h	Enthalpy
h_o	Total enthalpy (including dissociation)
$h\nu$	Planck's constant times electromagnetic frequency
k	Thermal conductivity
k_w	Surface catalytic reaction rate constant
Le	Lewis number
M	Mach number
M_a	Molecular weight of atoms
Pr	Prandtl number
\dot{q}	Heat transfer rate per unit area
R	Universal gas constant
Re	Reynolds number based on hemisphere radius
S	Parameter defined by Eq. (5)
Sc	Schmidt number
T	Temperature
U	Velocity
α	Degree of dissociation
β	Inviscid velocity gradient at stagnation point
γ	Specific heat ratio
γ_w	Recombination coefficient

θ	Angle between probe axis and normal to hemisphere surface
μ	Viscosity
ρ	Density
ϕ	Extent of recombination

SUBSCRIPTS

BL	Boundary layer (high Reynolds number) solution
chem	Contribution due to dissociation
e	Conditions at outer edge of boundary layer
f	Chemically "frozen", i. e. excluding chemical contribution
max	Maximum value (complete recombination)
o	Stagnation point conditions
w	Wall conditions
2	Conditions downstream of normal shock
∞	Free-stream conditions

SECTION I INTRODUCTION

It has been recognized for some time that a body traveling at hypersonic speeds through the upper atmosphere may experience a mechanism of heat transfer other than the purely molecular heat conduction process of conventional fluid mechanics. This will occur when the shock wave ahead of a body converts a portion of the flight kinetic energy into the chemical energy of dissociation of the air molecules. In this event, two driving mechanisms for heat transfer to the body become apparent; the temperature gradient across the boundary layer and the concentration gradient of atoms within the boundary layer. The relative importance of these two mechanisms in fixing the amount of heat transfer which will occur is determined by the conditions within the boundary layer and at the body surface.

If the boundary layer flow properties, particularly the density, are such that the characteristic time required for atom recombination is very much smaller than the time required for atom diffusion across the boundary layer, then the equilibrium boundary layer exists, in which the recombination is completed before the atoms can diffuse to the cold surface. In the other extreme, the "frozen" boundary layer case, the characteristic time for atom recombination is so large that no recombination can occur before the atoms have diffused to the surface. In these regimes, and in the intermediate regime where the characteristic times for diffusion and recombination are of comparable order of magnitude, the dimensionless combination of properties known as the Lewis number is of particular importance.

The dimensionless group $\rho c_p D/k$, commonly called the Lewis number, arises as a matter of convenience in the analysis of convective heat transfer from dissociated gases. It represents the ratio of the diffusivity of dissociated atoms to the thermal diffusivity of heat by conduction. For similar profiles of temperature and atom concentration across the boundary layer, and for a given total enthalpy at the edge of the boundary layer, the heat transfer rate is strictly dependent upon the enthalpy difference when $Le = 1$, regardless of the proportion of the enthalpy gradient associated with a temperature gradient or an atom concentration gradient. For, with $Le = 1$, energy will be transported across the boundary layer by both conduction and atom diffusion at the same rate per unit temperature gradient or concentration gradient. It will be observed that in the restriction of similar profiles of temperature and atom concentration, the condition of zero atom concentration at the solid surface is analogous to the zero temperature jump condition.

For the more general case, when the Lewis number is different from unity, the heat transfer rate is no longer simply dependent upon the total enthalpy difference across the boundary layer. The greater atom diffusion rate associated with a Lewis number greater than unity augments the transport of energy to the cold surface, whereas the smaller atom diffusion rate associated with a Lewis number less than unity retards the transport of energy to the surface. For most partially dissociated gases of aerodynamic interest, including air, the Lewis number is slightly greater than unity, the effect being to increase the heat transfer rate, say, on the order of 10 percent.

The preceding statements have been confined strictly to the case involving similar temperature and atom concentration profiles; that is, the atom concentration is zero at the cold surface. For a partially or completely frozen boundary layer, the case of zero atom concentration at the wall represents the limiting case of a surface which is fully catalytic to atom recombination; that is, all atoms which diffuse to the surface recombine there, depositing their chemical energy on the surface. In general, a surface will not be fully catalytic. Therefore, some of the atoms which reach the surface will not recombine there, resulting in a finite atom concentration at the surface. The obvious result, if the boundary layer is partially or completely frozen, is that a surface which is not fully catalytic will cause the heat transfer rate to be reduced because of the decrease in surface recombination and the resulting decrease in the atom concentration gradient. The condition of completely frozen boundary layer and completely non-catalytic surface represents the lower limit on the heat transfer, where the chemical contribution is zero.

The laminar heat transfer to the stagnation region of a blunt-nosed body in hypersonic flow has been treated theoretically by several investigators (Refs. 1 through 6). Lees (Ref. 1) considered only the equilibrium boundary layer and the completely frozen boundary layer with a fully catalytic surface. Approximate, closed-form solutions for these two cases were obtained from the boundary layer equations simplified on the basis of physical arguments. Fay and Riddell (Ref. 2) obtained numerical solutions to the boundary layer equations over homogeneous (gas-phase) recombination rates from equilibrium flow to frozen flow in the boundary layer. Again, these results apply only for the limiting case of a fully catalytic surface.

Goulard (Ref. 3) integrated the frozen laminar boundary layer equations and obtained a solution to the stagnation heat transfer problem with an arbitrary degree of catalytic activity at the surface. This was done simply by introducing a correction factor, ϕ , which is a function of the flow conditions, nose geometry, and wall catalytic reaction rate constant,

to account for the realistic condition in which the atom concentration at the wall is not zero. Rosner (Ref. 4) has suggested an expression for the frozen boundary layer stagnation heat transfer which is quite similar to the results of both Goulard and Fay and Riddell, while employing a more consistent use of the correction factor, ϕ , when the surface temperature cannot be neglected. This expression is considered in detail in a later section of this report.

Several other authors have treated analytically the problem of stagnation point heat transfer in hypersonic flow. Chung and Liu (Ref. 5) have developed an approximate analysis to predict the heat transfer to a noncatalytic surface. Their results were then generalized to apply to simultaneous gas-phase recombination and surface catalytic recombination. Inger (Ref. 6) has also presented an approximate theory of non-equilibrium stagnation point boundary layers with atom recombination at the surface.

Numerous other authors (Ref. 7) have investigated various facets of the effects of chemical kinetics in convective heat transfer. Nearly all of these investigations have been of a theoretical nature, and the principles involved in the theory are well understood. In fact, Spaulding (Ref. 8) has stated that "no mysteries now remain" in our ability to predict the effects of chemical reaction on heat transfer from gases.

On the other hand, the view taken by the present writer is that there has been far too little experimental verification of the existing theories on heat transfer from chemically reacting gases. This lack of verification is not surprising in view of the difficulties involved in making such measurements.

Rose and Stark (Ref. 9) have reported the results of shock tube measurements of stagnation point heat transfer in dissociated air. They obtained good agreement with the equilibrium boundary layer theory of Fay and Riddell (Ref. 2). The flow conditions were such that any non-equilibrium effects in the boundary layer and at the surface, if present at all, were very small. Busing (Ref. 10) obtained shock tube measurements of the stagnation point heat transfer to both catalytic and noncatalytic walls. Although his results showed a reduction in heat transfer with the noncatalytic surface, the size of the reduction was not nearly as large as expected.

The differential heat transfer to catalytic and noncatalytic surfaces in a steady-state, supersonic wind tunnel was measured by Rosner (Ref. 11) and by Winkler and Griffin (Ref. 12). A sizeable heat transfer difference was obtained in each investigation. These experiments,

however, were not designed to allow comparison of the results with an appropriate theory for heat transfer.

Hartunian and Thompson (Ref. 13) have reported preliminary measurements of catalytic and noncatalytic differential heat transfer in a low density shock tube. Their large (17-in.-diam) shock tube permits larger probes and greater test times than are usually possible with smaller, low pressure shock tubes.

The need for additional experimental data on nonequilibrium heat transfer with surface catalysis is clear. The available experimental results generally have not been compared with an appropriate theory (such as Fay-Riddell, Ref. 2) for predicting the absolute level of heat transfer. The usual procedure has been simply to show the percentage reduction in heat transfer caused by a noncatalytic wall, with little concern for the absolute values. It is fair to say that most experimental results of nonequilibrium heat transfer to catalytic and noncatalytic surfaces have been qualitative, not quantitative.

The purpose of this report is to present quantitative results of an experimental investigation of the heat transfer to blunt bodies, with both catalytic and noncatalytic surfaces, in nonequilibrium dissociated hypersonic flow. These experiments were performed in a small, continuous flow, low density hypersonic wind tunnel in operation at the von Karman Gas Dynamics Facility (VKF).

SECTION II FLOW CONDITIONS

2.1 THE WIND TUNNEL

The wind tunnel used in this investigation consists of the following major components, in streamwise order:

1. Direct current arc-heater (Thermal Dynamics U-50), with 40-kw power supply;
2. Settling section of variable size but normally of 3-in. diam and 6- to 10-in. length;
3. Aerodynamic nozzle of variable size with 0.10- to 0.75-in.-diam throat and 2.0- to 8.0-in.-diam exit;
4. A tank of 48-in. diam surrounding the test section and containing instrumentation and probe carrier;
5. Interchangeable diffuser;
6. Water-cooled heat exchanger;

7. Air-ejector of two stages; and
8. The VKF mechanical vacuum-pumping system.

A photograph of the tunnel is presented as Fig. 1.

Since this wind tunnel is used to study aerodynamic problems of low density, hypersonic flows, it is necessary that the tunnel flow conditions be known with a higher degree of accuracy than is common with arc-heated facilities normally used in heat transfer experiments. A survey of some of the techniques used in flow calibration and diagnosis is presented in Refs. 14 and 15. These techniques have been used in the present investigation to establish the test section flow conditions with what is believed to be a high degree of accuracy.

The wind tunnel is usually operated with nitrogen at reservoir pressures greater than one atmosphere and at a test section total enthalpy corresponding to an equilibrium temperature of about 3000°K. It has been shown (Ref. 15) that the gas, at this pressure and enthalpy, will approach thermodynamic equilibrium upstream of the nozzle throat provided the settling chamber is of sufficient length to allow complete mixing and recombination of the highly energetic species produced by the arc heater, where temperatures in excess of those required for nitrogen dissociation are present. Therefore, the number of nitrogen atoms in the test section of the nozzle is negligible at the usual tunnel operating conditions. However, when the tunnel is operated at a reservoir pressure much less than one atmosphere, there is an insufficient number of collisions within the reservoir to allow complete atom recombination upstream of the nozzle throat. Hence, a small fraction of the test section flow will be dissociated even when the average temperature is well below the dissociation level, resulting in a significant increase in the total enthalpy above the equilibrium value (cf, Ref. 15). It is this capability, together with the refined calibration procedures and the features of continuous operation, which makes this facility attractive for the study of heat transfer in dissociated nonequilibrium flow.

2.2 FLOW DIAGNOSIS

A wide variety of flow conditions involving nonequilibrium dissociation may be obtained in Tunnel L by proper choice of the nitrogen flow rate, total pressure, settling chamber geometry, and the nozzle throat area. The feasibility of the present investigation was demonstrated in a brief preliminary investigation* by the present author and

*These preliminary results are reported as an example in Ref. 16. They are qualitatively correct; however, the numerical values may be slightly revised in light of the present experiments.

a colleague, J. T. Miller. The same flow conditions used in this early investigation were selected for the present investigation. The nitrogen flow rate was 15.2 lb_m/hr at a measured reservoir pressure of 3.5 psia. A settling chamber with a diameter of 3 in. and nominal length of 8 in. was used. The aerodynamic nozzle had a throat diameter of 0.397 in. and a conical expansion section with a 15-deg half-angle.

2.2.1 Total Enthalpy Measurements

When the thermo-chemical flow conditions in a wind tunnel nozzle are not known *a priori*, it is then impossible to compute the total enthalpy of the flow from the usual measured quantities such as mass flow rate, total pressure, and throat area. The investigator must turn to a direct measurement of the total enthalpy in the test section.

The device used for this measurement in the present investigation is the total-enthalpy and mass-flow probe shown in Fig. 2. The probe consists of two concentric water-cooled jackets, separated by an air space to provide thermal insulation. Each jacket is knife-edged at the front to minimize the contact area for heat conduction between jackets and to provide the proper geometry to enable the bow shock to be "swallowed" when the probe is placed axially in the test section. The function of the inside jacket is to remove energy from the captured flow and deposit this energy in the cooling water, whose flow rate and temperature rise are measured. The total energy convected into the calorimeter is then the sum of the energy increase in the cooling water of the internal jacket and the residual energy of the gas leaving the calorimeter, as measured by a thermocouple.

The total enthalpy of the nozzle flow is obtained by dividing the total energy convected into the calorimeter by the mass flow captured by the calorimeter. If the bow shock is completely swallowed, the mass flow rate is simply the quantity $\rho_\infty U_\infty$ times the probe capture area. If the bow shock is not swallowed, the captured mass flow rate must be measured independently.

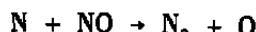
This probe was designed to allow an accurate measurement of the captured flow rate. The flow is directed from the probe to an evacuated vessel of known volume. The flow rate is determined by observing the pressure rise in the vessel during a measured time interval. The details of this procedure have been reported in Ref. 14. The measured flow rate was found to be unchanged when the time interval and the back pressure were varied over a wide range, indicating that the bow shock at the probe entrance was indeed swallowed.

Since it is virtually impossible to eliminate all internal paths for heat loss in a probe of this size in such an extreme environment, this device is an imperfect calorimeter and must be calibrated. The calibration procedure consisted of testing the probe in the flows from two other nozzles, operating at three flow conditions for which the total enthalpy is well known from other measurements. The probe measurements were found to be 7.8, 5.3, and 9.1 percent higher than the actual total enthalpy for the three flow conditions. The calibration correction factor used for the nonequilibrium flow condition was 7.4 percent, the average of the three deviations. Using this factor to adjust the probe measurement, the total enthalpy of the dissociated flow was found to be 1130 Btu/lbm.

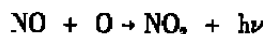
If it is further assumed that all of the total enthalpy tied up in non-equilibrium modes at the nozzle throat is caused by dissociation, i.e., vibration is in equilibrium at the nozzle throat, then the chemical energy of dissociation is computed to be 393 Btu/lbm. Since the dissociation energy for nitrogen is 14,270 Btu/lbm, the dissociation fraction, α , is found to be 0.0275.

2.2.2 Nitric Oxide Titration

In order to obtain an independent measurement of the nitrogen atom fraction in the test section, the nitric oxide light titration technique was used. This technique, first described by Spealman and Rodebush (Ref. 17) and discussed later in more detail by Kistiakowsky and Volpi (Ref. 18), is based on the fact that the reaction



is very fast compared with the reaction of nitrogen atoms with any other particles. The addition of nitric oxide to a stream containing nitrogen atoms is accompanied by a pronounced change in the emission spectrum, producing a change of colors from orange-yellow through pink and purplish-blue to colorless and then to whitish-green as increasing amounts of nitric oxide are added (Refs. 19 through 22). The titration end point, or the condition at which all of the nitric oxide is consumed by the nitrogen atoms, is just reached when the emission of light disappears. The titration end point is very sharply defined, since only a small increase in the nitric oxide flow rate will result in the whitish-green emission of the reaction



which occurs whenever nitric oxide is added in excess of the stoichiometric amount for reaction with nitrogen atoms. The mole flow rate of

nitrogen atoms is determined by measuring the nitric oxide flow rate at the titration end point, since the reaction occurs in equimolar proportions. Discussions of the merits of the nitric oxide titration technique may be found in Refs. 23 and 24.

The nitric oxide was injected into the test section through a stainless steel, uncooled, 1/4-in. -diam probe positioned on the axis of symmetry. The upstream end of the probe was closed. Several holes were drilled in the probe at a position about 1/2 in. behind the tip to permit a uniform radial injection of the nitric oxide.

It was found that the emission of light from the tank volume surrounding the high speed portion of the flow was very sensitive to the nitric oxide flow rate, while the colors produced in the high speed flow of nitrogen varied from point to point in the stream. This color variation undoubtedly resulted from the poor mixing obtained in the immediate vicinity of the injection probe, complicated by the possibility that the chemical reactions which produce the afterglow, even though very fast, were not completed near the probe. The emission of light in all parts of the tank volume outside the high speed stream indicated that a significant quantity of nitrogen atoms and nitric oxide molecules was reaching this area. It has been shown (Ref. 25) that there is a reverse flow along the walls of the convergent diffuser entrance section. This reverse flow has been observed by attaching tufts to the diffuser walls. It was also plainly visible during the whitish-green emission caused by excessive nitric oxide. Therefore, this reverse flow and mixing phenomenon is the mechanism by which the reacting species reach the outer volume of the tank.

With no nitric oxide injection into the stream, the yellow-orange Lewis-Rayleigh nitrogen afterglow was clearly visible when the room lights were darkened. This emission, which accompanies the homogeneous decay of nitrogen atoms (Refs. 22 and 26), filled the entire tank surrounding the test section. As a small amount of nitric oxide was injected into the flow, the emission inside the tank became darker in color and less intense until, at a particular nitric oxide flow rate, the visible emission was completely extinguished. A very minute increase in the nitric oxide flow rate resulted in a series of whitish-green flashes of light which traversed the entire volume of the tank in a random manner. A further increase in the nitric oxide flow rate caused the emission of the relatively intense whitish-green light continuously throughout the entire tank volume. The nitric oxide flow rate was measured at the condition where the light was extinguished, just prior to the appearance of the white flashes.

The results of the titration procedure, in terms of the measured nitrogen atom fraction, are presented in Fig. 3 for various probe positions in the test section. The upstream tip of the probe, located on the flow centerline, was moved axially to several stations in the test section near the nozzle exit. The measured nitrogen atom fraction decreased as the probe was moved downstream from the nozzle exit. Although this result is in the correct direction to account for atom recombination in the nozzle flow, the better explanation is found in the mixing process downstream of the probe and at the diffuser. Since the titration end point is determined by observing the color changes in the tank volume outside the primary flow region, the technique will be accurate only if the nitric oxide and nitrogen atoms and their products of reaction are well mixed at the diffuser entrance and are trapped in the reverse flow at the diffuser walls in the proper relative proportion. By injecting the nitric oxide at the tank wall instead of on the flow centerline, it was found that far less titrant gas was required to reach the apparent titration point. Therefore, since the overwhelming percentages of nitrogen atoms and titrant gas pass through the diffuser without being recirculated, the results of the technique are dependent upon the efficiency of the mixing process. The change in the probe location undoubtedly affects the mixing process and hence the measured atom fractions. Even though the titration technique must be considered only semi-quantitative in the present application, its results were very useful in increasing confidence in the atom fraction measurement obtained with the calorimeter probe. The calorimeter probe measurement of 0.0275 falls amazingly close to the center of the band of measurements shown in Fig. 3.

2.2.3 Impact Pressure Survey

The impact pressure probe is of major importance in flow calibration since the flow conditions can, in principle, be calculated from the measured impact and total pressures if the correct thermo-chemical flow model is known.

In this investigation the test section flow properties (density, velocity, and Mach number) were calculated from the results of an impact pressure survey in the test section. For this calculation it was assumed that the previously measured value of the dissociation fraction ($\alpha = 0.0275$) remained constant throughout the entire nozzle, while the molecular vibration mode was in equilibrium upstream of the throat and frozen downstream of the throat. This assumption is at least qualitatively correct since the number of collisions required for atom recombination is several orders of magnitude greater than the number required for vibrational relaxation.

As a further check on the validity of the assumed thermo-chemical flow model, use was made of a solution recently developed by Kinslow and

Miller, colleagues of the writer. This solution (Ref. 27) applies the basic equations for the conservation of mass, momentum, and energy to the one-dimensional adiabatic flow of an inviscid diatomic gas with finite vibrational relaxation and dissociation recombination rates. Together with the rate equation, these equations are solved by an iteration technique on a digital computer from any initial condition for the flow through a hypersonic nozzle. For the conditions measured in the test section in this investigation ($h_0 = 1130 \text{ Btu lb}_m$, $\alpha = 0.0275$), it was determined that the dissociation was indeed frozen throughout the nozzle, and that molecular vibration, while frozen downstream of the nozzle throat, was not too different from its equilibrium value upstream of the throat. Therefore, the assumed flow model was verified to be substantially correct, validating the flow property calculation procedure based on the measured impact pressures.

Some of the important flow parameters are given in Table I for several locations along the flow centerline.

2.3 BOUNDARY LAYER CONDITIONS

2.3.1 Re-Entry Simulation

The dissociation which may exist within the boundary layer around an actual re-entry vehicle is generated by the detached shock wave as it passes through the ambient atmosphere. If the flow field behind the shock wave is in equilibrium, then the highest possible amount of dissociation will have been produced. If the boundary layer flow remains in equilibrium, then the computation of the heat transfer for this case is straightforward since, for the cold-wall condition considered here, the effects of surface atom recombination are absent.

The more interesting (and difficult) situation occurs when the flow field behind the shock wave is not in equilibrium. In this case, the shock-induced dissociation will lag behind the equilibrium value up to the outer edge of the boundary layer. Then, if the boundary layer itself is not in equilibrium, at some point within the boundary layer the actual dissociation fraction will reach a maximum value and then decrease toward the wall. The computation of the heat transfer for this case is difficult because, in addition to the effects of wall recombination, the quantity of energy deposited in dissociation is unknown.

Exact duplication of the actual thermo-chemical re-entry model in a wind tunnel is difficult to achieve. In addition to the difficulties associated with obtaining the high temperatures necessary for shock-induced dissociation, the low densities required for a nonequilibrium boundary layer would result in a nonequilibrium nozzle expansion and a significant

amount of free-stream dissociation. Furthermore, the difficulties in experimentally determining the actual thermo-chemical state of the gas near the body appear formidable.

The alternative procedure for the wind tunnel simulation of re-entry is the production of a nonequilibrium dissociated free-stream flow, as was done in the present work. The total temperature corresponding to the translational, rotational, and vibrational degrees of freedom was about 1525 °K. Obviously there could be no additional dissociation produced through the shock region at this temperature, but the possibility of recombination in this region must be examined.

The question of gas-phase atom recombination in the stagnation region of blunt bodies at low Reynolds numbers has been considered by Goulard (Ref. 3), Grier and Sands (Ref. 28), Rosner (Ref. 29), Cheng (30), and Buckmaster (Ref. 31). Cheng assumed a single dissociation-recombination reaction of the type $N_2 + M \rightleftharpoons N + N + M$, where M represents a third body. He then calculated the value of the dissociation fraction through the shock layer for several values of Reynolds number. At the lowest Reynolds number considered, he found that both dissociation and recombination were negligible in the shock layer. As the degree of rarefaction decreased, the effect of dissociation in the outer portion of the shock layer became significant while recombination remained negligible. As pointed out by Buckmaster, this is primarily because recombination requires three-body collisions, which occur less frequently than the dissociation collision. At the highest Reynolds number considered by Cheng, which was higher than those of the present investigation, the gas-phase recombination was still negligible. Comparison of the present flow conditions with the numerical results of Rosner (Ref. 29) for a similar flow condition results in the same conclusion, that is, negligible recombination in the boundary layer. Furthermore, as Rosner points out, if recombination is not appreciable in the boundary layer itself, it will certainly be negligible in the entire shock layer region.

2.3.2 Second-Order Effects

In the low density regime in which the present experiments were conducted, the usual first-order boundary layer theory must be modified to consider second-order effects such as external vorticity, displacement, curvature, slip, and temperature jump. A number of investigators (Refs. 32 through 45) have considered one or more of these second-order effects using various techniques. Van Dyke (Ref. 46) has presented an excellent review and critical discussion of this subject. It is sufficient to state that the agreement between the several theories has not always been good. Similarly, the agreement between experiment and theory is

poor in many instances. Furthermore, there is some disagreement between experiments performed at different laboratories.

It is hoped that the experiments reported here will be welcomed not only by those whose main interests lie in the chemical-kinetic and surface effects of heat transfer but also by those who are concerned with the second-order effects in hypersonic boundary layers. Indeed, in many physical situations these two classes of problems will appear simultaneously.

SECTION III HEAT TRANSFER PROBES

The total heat transfer rate to the hemispherical noses of water-cooled, calorimeter-type probes was measured. This type probe, shown in Fig. 4, measures the steady-state, linear temperature drop along a conductor of known thermal conductivity and cross-sectional area. The steady-state heat transfer rate to the hemispherical nose is then calculated using Fourier's law. Since the conductor within the probe is shielded from the external flow, the heat losses are negligible. The probe is calibrated by applying a known heat input, and a calibration factor of unity is consistently obtained at the author's laboratory for this type probe.

In order to obtain data over a wider range of Reynolds numbers, three probes, with nose radii of 0.25, 0.50, and 0.75 in., were used. The hemispherical nose of each probe was machined from solid copper of high purity. This copper surface was used as the catalytic probe, with no surface preparation other than polishing with fine emery paper.

The same three probes were used to obtain the noncatalytic wall data. Two noncatalytic surfaces were tested. The first noncatalytic surface was ortho-phosphoric acid (H_3PO_4), applied to the copper surface with a brush, and allowed to dry under vacuum conditions. The second noncatalytic surface was a layer of silicon monoxide, evaporated onto the copper hemisphere. The thickness of this coating was estimated to be of the order of $2 \times 10^4 \text{ \AA}$ near the stagnation point, with the thickness decreasing with distance from the stagnation point. The additional thermal resistance resulting from these thin coatings was negligible.

The data for any single probe and surface were not all obtained consecutively, but the probe-surface combinations were tested in a somewhat random pattern. That is, each probe was coated and cleaned

numerous times in the data gathering process. The data repeatability was quite satisfactory for the copper surface. For the noncatalytic surfaces, there was some scatter in the data, which can be attributed to the inability to obtain identical surface catalytic properties with successive preparations of the surfaces.

SECTION IV EXPERIMENTAL RESULTS

4.1 TREATMENT OF DATA

The most common method of presenting experimental heat transfer data at low Reynolds numbers is to normalize the results with the first-order boundary layer theory applicable at high Reynolds numbers, that is, to present the ratio \dot{q}/\dot{q}_{BL} . The correlation equation of Rosner (Ref. 47) was selected for the calculation of \dot{q}_{BL} :

$$\dot{q}_o = 0.763 \left(\frac{\rho_w \mu_w}{\rho_e \mu_e} \right)^{0.1} \left(\beta \rho_e \mu_e \right)^{0.5} \left(Pr \right)^{-0.6} \Delta h \left\{ 1 + \phi \left[\left(Le \right)^{0.6} - 1 \right] \frac{\Delta h_{chem,max}}{\Delta h} \right\} \quad (1)$$

where the magnitude of the enthalpy difference across the boundary layer is

$$\Delta h = (h_o - h_{f,w}) - (1 - \phi) \Delta h_{chem,max} \quad (2)$$

This equation is of a form similar to the correlation equations of Fay and Riddell (Ref. 2) and Goulard (Ref. 3) for the frozen boundary layer, while differing from Rosner's earlier result (Ref. 4) only by the inclusion of the factor accounting for variable $\rho \mu$. The extent of recombination ϕ , defined by

$$\phi = \frac{\alpha_e - \alpha_w}{\alpha_e} \quad (3)$$

has been generalized by Rosner to include recombination in the gas phase as well as at the body surface. For a completely frozen boundary layer, ϕ can be reduced to the simple form

$$\phi = \frac{1}{1 + \frac{S}{k_w}} \quad (4)$$

using the notation of Goulard (Ref. 3). The constant k_w , known as the catalytic activity or surface catalytic reaction rate constant, is a property having the dimensions of velocity. The quantity S , which is a measure of the diffusion velocity in the boundary layer, is given by

$$S = 0.763 \left(\beta \rho_e \mu_e \right)^{0.5} \left(Sc \right)^{-0.6} \rho_w^{-1} \quad (5)$$

The Prandtl, Schmidt, and Lewis numbers were taken as constants, since the uncertainty of their correct values is probably greater than

their variation across the boundary layer. The Prandtl number was taken as 0.71, a value well accepted in the literature. Following Lees (Ref. 1), the Schmidt number was taken to be 0.49. The Lewis number, or the ratio of the Prandtl number to the Schmidt number, was then calculated to be 1.45. This value is in agreement with the work of Brokaw (Ref. 48). (Many writers have used the value 1.4 for the Lewis number, possibly because of the excellent publicity this number has received from other sources.)

The inviscid velocity gradient at the nose was calculated using the equation of Probstein (Ref. 49) for modified Newtonian flow:

$$\beta = \frac{U_{\infty}}{a} \left[\frac{\rho_{\infty}}{\rho_1} \left(2 - \frac{\rho_{\infty}}{\rho_1} \right) \right]^{0.5} \quad (6)$$

Potter and Bailey (Ref. 50) have found that the modified Newtonian pressure distribution is accurate, even at these low Reynolds numbers, in the region $0 < \theta < 70$ deg for highly cooled hemispheres.

Since Eq. (1) predicts only the stagnation point heat flux, the heat transfer distribution around the hemisphere must be known in order to predict the total heat transfer to the hemisphere for comparison with the experimental results. The heat transfer distribution given by Lees (Ref. 1) was used for this calculation. The assumptions implicit within Lees' derivation include a thin boundary layer with no second-order effects, cool wall, Prandtl and Lewis numbers of unity, constant $\rho\mu$, and chemical equilibrium at every point in the boundary layer. Obviously, some of these assumptions are inaccurate for the present experiments, and the resulting effects on the heat transfer distribution must be considered.

Kemp, Rose, and Detra (Ref. 51), using the "local similarity" concept and an extension of the ideas used by Fay and Riddell (Ref. 2), derived another expression for the ratio of local heat transfer rate to stagnation point rate. They showed that the effect of considering $\rho\mu$ variable was practically equal and opposite to the effect of using 0.71 instead of unity for the Prandtl number. They further showed that the effect of non-unity Lewis number was small for Lewis numbers of the order of 1.4 and that the effect of a nonequilibrium boundary layer was small provided the wall was fully catalytic. Dorrance (Ref. 52) has shown that the results of Kemp, Rose, and Detra are equivalent to the distribution of Lees multiplied by a factor which is a function only of a pressure gradient parameter. It is further shown that for most body shapes of practical interest (including hemispheres) this factor is very near unity. The shock tube data of Kemp, Rose, and Detra agree equally well

with their own predictions and the distribution of Lees. In addition; Vidal and Wittliff (Ref. 53) and Hickman (Ref. 54) have presented data at low Reynolds numbers which are in good agreement with the distribution of Lees for hemispheres. Their results show that the heat transfer distribution is insensitive to Reynolds number for hypersonic flow.

The above considerations strongly support the use of Lees' heat transfer distribution in the treatment of the present data for a fully catalytic surface. However, for the "noncatalytic" surfaces, there are no such firm grounds available to justify its use. Nonetheless, it will be used for these surfaces also, since no better information exists.

4.2 SURFACE BEHAVIOR

Before the experimental results are presented, it is appropriate to comment on the apparent behavior of the surfaces when exposed to the tunnel flow. The change of surface catalytic properties with time during the test runs was evident to some degree in almost all cases and was of particular concern with the coated surfaces.

The test procedure generally followed was to begin the measurements with the probe located at the station farthest downstream from the nozzle, where the heating rate was least. After this measurement was obtained, the probe was moved from station to station toward the nozzle, until the final station at the nozzle exit plane was reached. Then this traverse was repeated, usually in both forward and reverse directions.

The bare copper surface exhibited an increase of about 15 percent in total heat transfer at the initial station after one complete traverse of the test section. The time required for a complete traverse of the test section was approximately twenty minutes. After this first traverse of the test section, there was no observable change in the heat transfer rate at a particular station no matter how many additional traverses were made.

The fact that some change in the probe surface had occurred was evident from visual inspections. The probe, which initially had a shiny appearance from the polishing with emery paper, had distinctly changed in appearance following a series of measurements in the wind tunnel. The altered surface appeared dark and dull to the eye, and it appeared that this new surface was actually a thin deposit of some material. A spectrographic analysis of this deposit revealed the characteristic lines of copper, possibly in an oxide form.

The most probable source of this copper deposit is the copper anode in the arc heater. Because of the action of the arc column, the anode does erode and must be replaced periodically, say, once or twice a week. This erosion is so slow that the flow contamination is completely negligible for most aerodynamic measurements. On the other hand, when the measurement is sensitive to minute changes in the properties of the body surface, as in catalytic heat transfer measurements, a thin deposit of copper could significantly alter the microscopic surface structure of the body as seen by the gas particles themselves, thereby affecting the catalytic properties at the wall.

It is conjectured that in the present experiments a very thin layer of copper was deposited on the probe surface, leaving the surface rather porous and "rough" on the microscopic scale as compared with the original "smooth" surface. This "microscopically rough" surface, with its peaks and crevices, would contain a greater effective surface area and would have the ability to "adsorb" gas particles for longer periods of time, thereby enhancing the effective catalytic properties of the surface. Since copper is known to have good catalytic surface properties, the properties of this "roughened" copper surface should be excellent for catalytic recombination of atoms.

The surfaces coated with silicon monoxide and ortho-phosphoric acid exhibited the same increase in heat transfer rate with time as did the bare copper surface, except that the change did not stop after the first traverse of the test section, but continued with each traverse until the heat transfer rates to the bare copper were approached. This degeneration of the noncatalytic surface was apparently caused by the deposition of copper rather than the erosion of the surface coating, since the electrical insulating property of the silicon monoxide was the same before and after each run.

Since it was intended for the bare copper probe to demonstrate the effects of a highly catalytic surface, those measurements obtained during the initial traverse of the test section were discarded. Only those measurements obtained after the heat transfer rates became stable are included in this report. Likewise, the purpose of the coated probes was to provide measurements for a highly noncatalytic surface. Hence, only those measurements taken during the first traverse of the test section are included in this report. Even these first measurements include some effect of the changing surface properties caused by the forming layer of copper. The extent of this effect will be discussed when the data are presented.

The observed variation in the catalytic properties of these surfaces is not surprising in view of the experience reported by others. In

particular, Prok (Refs. 55 and 56) has found that surface catalytic properties of metals and metallic oxides are strongly dependent on the type of surface preparation as well as the duration of exposure to atomic species. He has also found that the thickness of an evaporated film and the type of substrate were quite important in surface catalysis. Also, Myerson (Ref. 57) reported that the catalytic efficiency of silver to oxygen atom recombination was initially a direct function of its duration of exposure to atomic oxygen fluxes. Hartunian and Thompson (Ref. 13) also found that pre-exposure of their probes to dissociated flow was necessary to produce reliable data.

4.3 EFFECT OF FINITE CATALYTICITY

Although a number of independent investigators have reported values of surface catalytic properties in the literature, Rosner (Ref. 58) has correctly cautioned against the use of these recombination coefficients for the composite conditions likely to be met in aerodynamic practice. Therefore, the recombination coefficients for the surfaces used in the present investigation were not known *a priori*, and, indeed, a significant portion of the data analysis consisted of determining the proper values to be used in comparing the experimental results with theory.

Thus far, two parameters which can be related to wall catalytic properties have been introduced. These are the extent of recombination, ϕ , and the surface reaction rate constant, k_w , related by Eq. (4). The limiting case of "complete" recombination, $\phi = 1$, corresponds to an infinite value of k_w , while the case of zero wall recombination, $\phi = 0$, corresponds to $k_w = 0$. For finite (realistic) values of k_w , the heat transfer rates will fall between these two limiting cases. In order to show the effect of finite values of k_w , calculations have been made using Eqs. (1) through (6) with the present flow properties for k_w values of 10^2 , 10^3 , 10^4 , and 10^5 cm/sec. The results of these calculations are compared with the limiting case $\phi = 1$ in Fig. 5. It is evident that a surface with k_w near 10^2 cm/sec would behave essentially as a completely noncatalytic surface, whereas a surface with k_w near 10^5 cm/sec would act essentially as a "fully catalytic" surface. Only for values of k_w between these limits would the effects of finite atom recombination be detected.

A third catalytic parameter which is of interest is the recombination coefficient, γ_w , defined as the ratio of the actual frequency of surface encounters leading to recombination to the total interfacial collision frequency for atoms. In other words, γ_w is the probability that an atom will recombine upon striking the wall. The recombination coefficient is dimensionless and has a microscopic interpretation, as opposed to the phenomenological interpretation of the surface reaction rate constant, k_w .

With the assumption of a Maxwellian velocity distribution for the atoms striking the surface, the relation between γ_w and k_w has been given by Goulard (Ref. 3) and Rosner (Ref. 59) as

$$k_w = \gamma_w \left(\frac{RT_w}{2\pi M_a} \right)^{1/2} \quad (7)$$

Since the upper limit of γ_w is unity, there will be a finite upper limit to k_w , according to Eq. (7), for each wall temperature. Therefore, the limiting case of "complete recombination", with $\phi = 1$ and k_w infinite, is not realistic in the strict sense. This can be seen in Fig. 5, where the heat transfer rates for several values of γ_w are compared with the case $\phi = 1$. The effect of using $\gamma_w = 1$ instead of $\phi = 1$ is to reduce the predicted heat transfer results by a few percent. In the correlation of experimental measurements, however, the difference between the cases $\phi = 1$ and $\gamma_w = 1$ may not be of great significance when the usual precision of heat transfer measurements is considered.

4.4 RESULTS FOR COPPER SURFACES

The measured total heat transfer rates to the copper surfaces are compared in Fig. 6 with the values calculated from Eq. (1) and Lees' distribution. The calculations were made assuming "complete recombination" at the surface, that is, $\phi = 1$. Also presented in the figure are the \dot{q}/\dot{q}_{BL} ratios predicted by the second-order theories of Cheng (Ref. 30) and Van Dyke (Ref. 41). The location of the curve representing Van Dyke's theory is generally typical for several other second-order boundary layer theories. The theory of Cheng is unique in that it predicts a higher heat transfer rate than most other theories; yet it approaches the free-molecule limit as the Reynolds number decreases.

There is excellent agreement between the experimental data and the theory of Cheng under the simplifying assumption $\phi = 1$. The indication is that the bare copper surface, when exposed to the tunnel flow long enough for the transient surface effects to disappear, is an extremely efficient catalyst to nitrogen atom recombination.

Since it was stated in the previous section that the more realistic case of full recombination is represented by $\gamma_w = 1$ instead of $\phi = 1$, these same experimental data are compared with the theory for the case $\gamma_w = 1$ in Fig. 7. Under this condition, the calculated values of ϕ range between 0.861, at the lowest Reynolds number, and 0.948 at the highest Reynolds number. The effect is to increase the values of \dot{q}/\dot{q}_{BL} slightly, since \dot{q}_{BL} would be decreased according to Fig. 5.

The data presented in Fig. 7 for the case $\gamma_w = 1$ fall slightly on the high side of Cheng's curve, but they are in no less agreement with the theory than are the data of Fig. 6 for $\phi = 1$. It is of interest to note that if k_w were calculated from the expression given by Cheng (Ref. 30)

$$k_w = \frac{2\gamma_w}{2 - \gamma_w} \left(\frac{RT_w}{2\pi M_a} \right)^{\frac{1}{2}} \quad (8)$$

instead of using Eq. (7), then, with $\gamma_w = 1$, the data would fall approximately half-way between their respective locations on Figs. 6 and 7, thus coinciding with Cheng's curve.

The experimental uncertainty in these measurements is estimated to be about ± 5 percent, mainly because of the probable uncertainty in the total enthalpy measurement and the use of Lees' distribution. The observable experimental scatter is also of this same order. It is felt that the data as presented in Fig. 7 represent the best comparison with theory since this figure does represent the most realistic catalytic surface condition. Certainly within the limits of experimental accuracy, the bare copper surface behaved as a fully catalytic surface, with $\gamma_w = 1$.

4.5 RESULTS FOR COATED SURFACES

The measured heat transfer rates to the surfaces coated with silicon monoxide and ortho-phosphoric acid are presented in Fig. 8. These results have been normalized with the values predicted by multiplying the results of Eq. (1), with $\phi = 1$, by the values of \dot{q}/\dot{q}_{BL} obtained from Cheng's second-order theory. Also presented in the figure are lines representing constant values of k_w and γ_w . The results for the bare copper surfaces, if presented in this figure, would lie between the top margin of the figure and the line $\gamma_w = 1.0$.

There is a marked reduction in heat transfer with the coated surfaces, being as much as 30 to 40 percent at the lowest Reynolds numbers. The upward trend in these data with increasing Reynolds number, evident in Fig. 8, would be expected to follow the slope of lines representing constant values of γ_w if there were no change in the surface catalytic properties during the run. The amount by which the actual slope of the data from a particular traverse of the test section exceeds the slope of a typical line representing constant γ_w , say $\gamma_w = 0.1$, is a measure of the effect of the changing surface properties with increasing exposure time. From Fig. 8, this effect is responsible for about ten percent of increase in heat transfer, during one test section traverse, above the increase which would result from the condition of constant γ_w .

These results clearly indicate the reduction in heat transfer which is possible in the frozen boundary layer regime when a noncatalytic surface is employed. Typically, values of the recombination coefficient γ_w range between 0.01 and 0.1, compared with 1.0 for the catalytic surfaces. The large scatter in the data results from the inability to obtain repeatable surface properties each time a surface was prepared.

It is interesting to note that the initial measurements with a freshly polished copper probe, taken at the lowest Reynolds number before prolonged tunnel exposure, were about 15 percent below the final steady-state values, corresponding (from Fig. 8) to a value of γ_w of roughly 0.6. This value is in good agreement with the results of Ammann (Ref. 60) for nitrogen atom recombination on copper.

4.6 COMPARISON WITH PREVIOUS MEASUREMENTS

Experimental data for local stagnation point heat transfer at low Reynolds numbers have been reported by several investigators (Refs. 53, 54 and 61 through 66). As previously stated, there have been some discrepancies between experiments from different laboratories. It is hoped that the present results will aid in the reconciliation of these discrepancies.

Ferri and co-workers (Ref. 62) have presented experimental data for the vorticity interaction regime for stagnation temperatures of 1600 and 2300 °R. These data, when presented in the form \dot{q}/\dot{q}_{BL} , show an increasing vorticity effect for increasing stagnation temperature. These data are in general agreement with the theory of Ref. 62 and also with the theory of Cheng, with both experiment and theory displaying a vorticity effect at much higher Reynolds numbers than predicted by other second-order theories.

Other measurements for the vorticity interaction regime have been reported by Hickman (Ref. 54). These measurements, obtained at a stagnation temperature corresponding to room temperature, are in reasonable agreement with the theory of Van Dyke and, therefore, indicate a much smaller vorticity effect than was observed by Ferri et al. Even though the data of Hickman and Ferri et al. do not agree, they are consistent in the sense that they show an increasing vorticity effect with increasing stagnation temperature.

As the Reynolds number is further decreased below those corresponding to the vorticity interaction regime, viscous effects in the layer between the shock and the body become important. Ferri and Zakkay (Ref. 63) have also reported experimental measurements in this viscous

layer regime for a stagnation temperature of 2100°R. These results are in agreement with the earlier data of Ferri et al. and show a decrease in \dot{q}/\dot{q}_{BL} in accord with the prediction of Cheng.

Potter and Miller (Ref. 66) have also reported measurements obtained earlier in the same wind tunnel used in the present measurements. Their measurements were also obtained in nitrogen, but at a higher stagnation pressure so that the flow contained no dissociation. These data are in good agreement with the Cheng theory presented in the normalized form as in Fig. 9.

Shock tunnel measurements at low Reynolds numbers have been reported by Vidal and Wittliff (Ref. 53). There is considerable scatter in these measurements and they could be used equally to support all theoretical predictions in the vorticity interaction regime. At the lowest Reynolds numbers, the data are in general agreement with Cheng's theory when the enthalpy associated with the free-stream atom concentration is neglected. Although the models used were presumed to have completely noncatalytic surfaces, some of the observed scatter could be caused by a variation in surface catalytic properties similar to that observed in the present investigation.

The data of Ferri et al. (Refs. 62 and 63) and Potter and Miller (Ref. 66) are reproduced in Fig. 9. These data may be compared with the present results given in Fig. 7. Agreement between the data in these two figures is relatively good.

SECTION V CONCLUSIONS

This report has presented the details and results of an experimental investigation of heat transfer in nonequilibrium dissociated hypersonic flow with surface catalysis and second-order boundary layer effects. This section is devoted to an enumeration of the significant observations made during the investigation and conclusions drawn from the investigation.

Since a significant effort was devoted to calibration of the nozzle flow, two observations concerning the flow diagnosis will be made. First, the combination mass-flow and total-enthalpy probe, although not entirely free from error, provided a satisfactory means of determining locally the total enthalpy of the flow. Secondly, the nitric oxide titration technique proved to be a useful method of determining the free-stream atom concentration, even in high speed flows.

The major observations and conclusions from the results of the experimental heat transfer measurements are summarized as follows:

1. The bare copper surfaces exhibit an initial recombination coefficient of about 0.6. The surface recombination increases rapidly with time until no further time-dependence is observed. At this steady-state condition, surface recombination is virtually complete, that is, $\gamma_w = 1$. This transient effect is attributed to an enhancing of the microscopic surface catalytic properties owing to the formation of a fine deposit of copper on the probe surface.
2. The experimental results for copper surfaces, normalized by the values computed from Rosner's stagnation point heat transfer equation assuming $\gamma_w = 1$, are in agreement with the thin shock theory of Cheng. Also, they are in agreement with the experimental measurements of Ferri and Zakkay.
3. A significant reduction in heat transfer to a noncatalytic surface has been demonstrated. The coated surfaces used in this investigation were highly susceptible to catalytic property changes with time of exposure.
4. The use of differential catalytic probes for determining free-stream atom concentrations is currently under study at several laboratories. The transient surface effects observed in this investigation point out a potentially serious limitation in the use of such probes to measure absolute values of atom concentration. To overcome this difficulty, surfaces must be used which retain known catalytic properties over long exposure periods.
5. The results of this investigation have by no means ended the need for additional experimental study of heat transfer with surface atom recombination and low density effects. To the writer's knowledge, this effort represents the first instance where combined surface atom recombination and second-order boundary layer effects have been studied experimentally.

REFERENCES

1. Lees, Lester, "Laminar Heat Transfer Over Blunt-Nosed Bodies at Hypersonic Flight Speeds." Jet Propulsion, Vol. 26, No. 4, April 1956, pp. 259-269.

2. Fay, J. A. and Riddell, F. R. "Theory of Stagnation Point Heat Transfer in Dissociated Air." Journal of the Aeronautical Sciences, Vol. 25, No. 2, Feb. 1958, pp. 73-85, 121.
3. Goulard, R. J. "On Catalytic Recombination Rates in Hypersonic Stagnation Heat Transfer." Jet Propulsion, Vol. 28, No. 11, Nov. 1958, pp. 737-745.
4. Rosner, Daniel E. "Similitude Treatment of Hypersonic Stagnation Heat Transfer." ARS Journal, Vol. 29, No. 3, March 1959, pp. 215-216.
5. Chung, P. M. and Liu, S. W. "An Approximate Analysis of Simultaneous Gas-Phase and Surface Atom Recombination For Stagnation Boundary Layer." Aerospace Corp. Report No. TDR-169(3230-12)TN-4, November 1962.
6. Inger, George R. "Nonequilibrium-Dissociated Stagnation Point Boundary Layers With Arbitrary Surface Catalycity." Aerospace Corp. Report No. ATN-63(9206)-3, January 1963.
7. Rosner, Daniel E. "Bibliography - Chemical Kinetic Effects in Convective Heat Transfer." AIAA Preprint 63114, AIAA-ASME Hypersonic Ramjet Conference, April 23-25, 1963.
8. Spaulding, D. B. "Heat Transfer From Chemically Reacting Gases." Modern Developments in Heat Transfer, Ed. by Warren Ibele, Academic Press, 1963, pp. 19-64.
9. Rose, P. H. and Stark, W. I. "Stagnation Point Heat-Transfer Measurements in Dissociated Air." Journal of the Aeronautical Sciences, Vol. 25, No. 2, Feb. 1958, pp. 86-97.
10. Busing, J. R. "A Preliminary Experimental Investigation of the Effect of Surface Catalytic Efficiency on Stagnation Point Heat Transfer." College of Aeronautics, Cranfield, Note No. 123, January 1962.
11. Rosner, Daniel E. "Diffusion and Chemical Surface Catalysis in a Low-Temperature Plasmajet." ASME J. Heat Transfer, Vol. 84, No. 4, Nov. 1962, pp. 386-394.
12. Winkler, Ernest L. and Griffin, Roy N., Jr. "Effects of Surface Recombination on Heat Transfer to Bodies in a High Enthalpy Stream of Partially Dissociated Nitrogen." NASA TN D-1146, Dec. 1961.
13. Hartunian, R. A. and Thompson, W. P. "Nonequilibrium Stagnation Point Heat Transfer Including Surface Catalysis." AIAA Preprint 63-464, AIAA Conference on Physics of Entry Into Planetary Atmospheres, Aug. 26-28, 1963.

14. Potter, J. L., Arney, G. D., Kinslow, M., and Carden, W. H. "Gasdynamic Diagnosis of High-Speed Flows Expanded From Plasma States." IEEE Transactions on Nuclear Science, Vol. NS-11, No. 1, Jan. 1964, pp. 145-157.
15. Potter, J. L., Arney, G. D., Carden, W. H. and Kinslow, M. "Irreversible Flow in Reservoir and Throat Sections of Wind Tunnels With Constricted-Arc Heaters." Arc Heaters and MHD Accelerators For Aerodynamic Purposes, AGARDograph 84, Sept. 1964, pp. 379-412.
16. Potter, J. Leith. "Hypersonic Flight Simulation: Aerodynamics." Presented at the Conference on the Role of Simulation in Space Technology, Virginia Polytechnic Institute, Blacksburg, Virginia, August 17-21, 1964.
17. Spealman, M. L. and Rodebush, W. H. "The Reactions of Some Oxides of Nitrogen With Atomic Oxygen and Nitrogen." J. American Chemical Society, Vol. 57, Aug. 1935, pp. 1474-1476.
18. Kistiakowsky, G. B. and Volpi, G. G. "Reactions of Nitrogen Atoms. I. Oxygen and Oxides of Nitrogen." J. Chemical Physics, Vol. 27, No. 5, Nov. 1957, pp. 1141-1149.
19. Kaufman, Frederick and Kelso, John R. "Excitation of Nitric Oxide by Active Nitrogen." J. Chemical Physics, Vol. 27, No. 5, Nov. 1957, pp. 1209-1210.
20. Kaufman, Frederick and Kelso, John R. "Vibrationally Excited Ground-State Nitrogen in Active Nitrogen." J. Chemical Physics, Vol. 28, No. 3, March 1958, p. 510-511.
21. Kaufman, Frederick. "Origin of Afterglows in Mixtures of Nitrogen and Oxygen." J. Chemical Physics, Vol. 28, No. 5, May 1958, p. 992.
22. Harteck, Paul, Reeves, Robert R., and Mannella, Gene. "Rate of Recombination of Nitrogen Atoms." J. Chemical Physics, Vol. 29, No. 3, Sept. 1958, pp. 608-610.
23. Fontijn, A., Rosner, D. E., and Kurzius, S. C. "Chemical Scavenger Probe Studies of Atom and Excited Molecule Reactivity in Active Nitrogen From a Supersonic Stream." Canadian J. Chemistry, Vol. 42, No. 11, Nov. 1964, pp. 2440-2450.
24. Back, R. A. and Mui, J. Y. P. "The Reactions of Active Nitrogen With N¹⁵O and N₂¹⁵." J. Physical Chemistry, Vol. 66, July 1962, pp. 1362-1364.

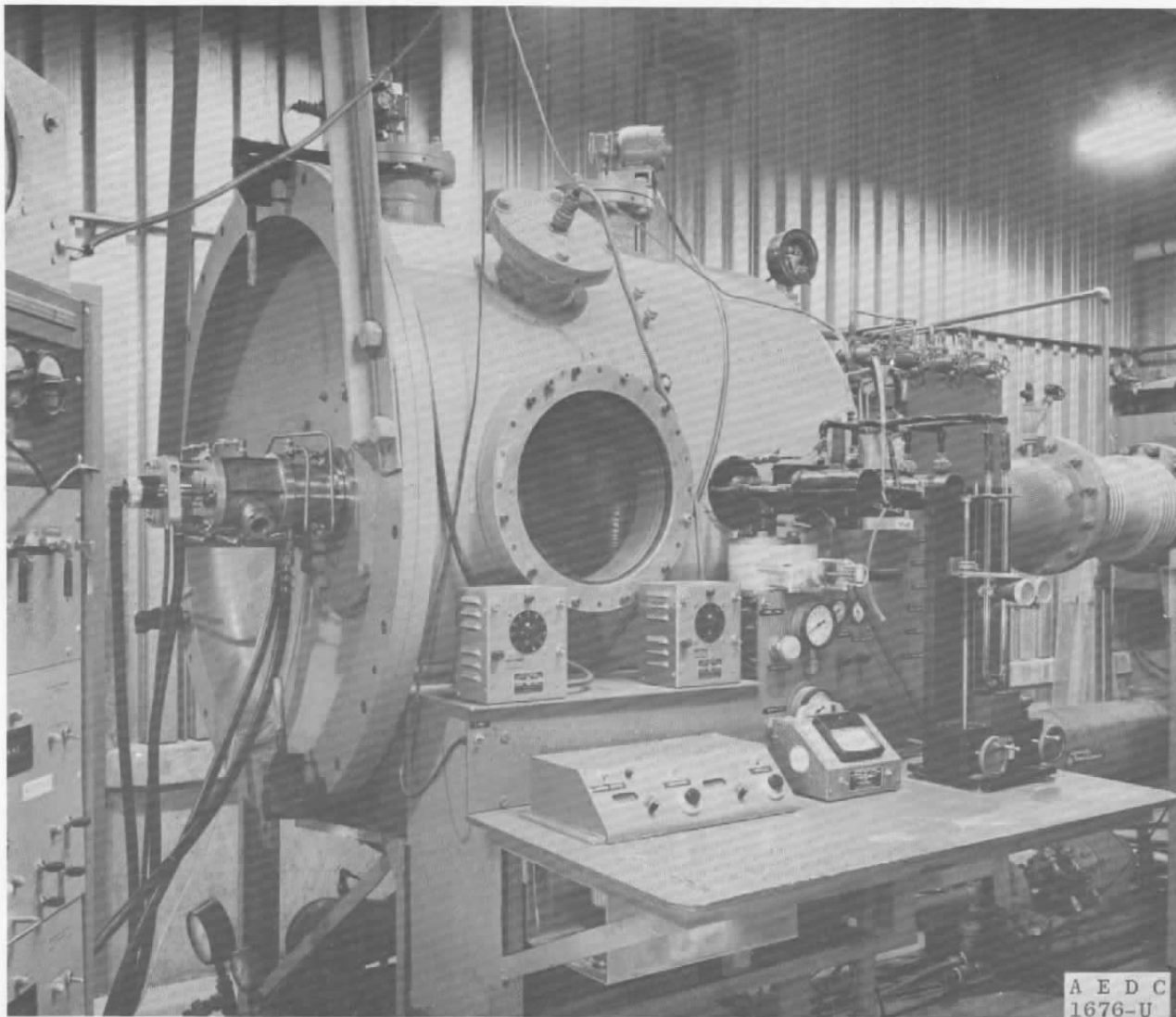
25. Boylan, D. E. "An Experimental Study of Diffusers in an Open-Jet, Low-Density, Hypersonic Wind Tunnel." AEDC-TDR-64-47 (AD 434380), April 1964.
26. Kelly, Roger and Winkler, C. A. "The Kinetics of the Decay of Nitrogen Atoms as Determined From Chemical Measurements of Atom Concentrations as a Function of Pressure." Canadian J. Chemistry, Vol. 37, 1959, pp. 62-78.
27. Kinslow, Max and Miller, J. T. "The Nonequilibrium Expansion of a Diatomic Gas Through a Convergent-Divergent Nozzle." AEDC-TR-65-103, June 1965.
28. Grier, Norman T. and Sands, Norman, "Regime of Frozen Boundary Layers in Stagnation Region of Blunt Reentry Bodies." NASA TN D-865, May 1961.
29. Rosner, Daniel E. "Catalytic Probes For the Determination of Atom Concentrations in High Speed Gas Streams. ARS Journal, Vol. 32, No. 7, July 1962, pp. 1065-1073.
30. Cheng, H. K. "The Blunt-Body Problem in Hypersonic Flow at Low Reynolds Number." Cornell Aeronautical Laboratory Report No. AF-1285-A-10, June 1963.
31. Buckmaster, J. D. "The Effects of Ambient Dissociation on Frozen Hypersonic Stagnation Flow." AEDC-TDR-64-142 (AD 601652), June 1964.
32. Hayes, Wallace D. and Probstein, Ronald F. Hypersonic Flow Theory, Academic Press, New York, 1959, p. 372.
33. Rott, Nicholas and Lenard, Michael. "Vorticity Effect on the Stagnation-Point Flow of a Viscous Incompressible Fluid." Journal of the Aerospace Sciences, Vol. 26, No. 8, Aug. 1959, pp. 542-543.
34. Kemp, Nelson H. "Vorticity Interaction at an Axisymmetric Stagnation Point in a Viscous Incompressible Fluid." Journal of the Aerospace Sciences, Vol. 26, No. 8, Aug. 1959, pp. 543-544.
35. Hoshizaki, H. "Shock-Generated Vorticity Effects at Low Reynolds Numbers." Lockheed Missiles and Space Division, LMSD-48381, Jan. 1959.
36. Herring, T. K. "The Boundary Layer Near the Stagnation Point in Hypersonic Flow Past a Sphere." Journal of Fluid Mechanics, Vol. 7, No. 2, Feb. 1960, pp. 257-272.

37. Probstein, Ronald F. and Kemp, Nelson H. "Viscous Aerodynamic Characteristics in Hypersonic Rarefied Gas Flow." Journal of the Aerospace Sciences, Vol. 27, No. 3, March 1960, pp. 174-192, 218.
38. Ho, H. T. and Probstein, Ronald F. "The Compressible Viscous Layer in Rarefied Hypersonic Flow." Rarefied Gas Dynamics, edited by L. Talbot, Academic Press, New York, 1961, pp. 525-552.
39. Ferri, Antonio, Zakkay, Victor and Ting, Lu. "Blunt-Body Heat Transfer at Hypersonic Speed and Low Reynolds Numbers." Journal of the Aerospace Sciences, Vol. 28, No. 12, Dec. 1961, pp. 962-971, 991.
40. Cheng, H. K. "Hypersonic Shock-Layer Theory of the Stagnation Region at Low Reynolds Number." Proc. Heat Transfer and Fluid Mechanics Institute, Stanford University Press, June 1961, pp. 161-175.
41. Van Dyke, Milton, "Second-Order Compressible Boundary Layer Theory with Application to Blunt Bodies in Hypersonic Flow." Hypersonic Flow Research, Edited by F. Riddell, Academic Press, New York, 1962, pp. 37-80.
42. Lenard, M. "Stagnation Point of a Variable Property Fluid at Low Reynolds Numbers." Ph.D. Thesis, Cornell University, Ithaca, N.Y., Sept. 1961.
43. Maslen, S. H. "Second-Order Effects in Laminar Boundary Layers." AIAA Journal, Vol. 1, No. 1, Jan. 1963, pp. 33-40.
44. Levinsky, E. S. and Yoshihara, H. "Rarefied Hypersonic Flow Over a Sphere." Hypersonic Flow Research, Edited by F. Riddell, Academic Press, New York, 1962, pp. 81-106.
45. Davis, R. T. and Flugge-Lotz, I. "The Laminar Compressible Boundary Layer in the Stagnation-Point Region of an Axisymmetric Blunt Body Including the Second-Order Effect of Vorticity Interaction." International Journal of Heat and Mass Transfer, Vol. 7, No. 3, March 1964, pp. 341-370.
46. Van Dyke, Milton. "A Review and Extension of Second-Order Hypersonic Boundary-Layer Theory." Rarefied Gas Dynamics, Vol. II, Edited by J. A. Laurmann, Academic Press, New York, 1963, pp. 212-227.
47. Rosner, Daniel E. "Scale Effects and Correlations in Nonequilibrium Convective Heat Transfer." AIAA Journal, Vol. 1, No. 7, July 1963, pp. 1550-1555.
48. Brokaw, Richard S. "The Lewis Number". Progress in International Research on Thermodynamic and Transport

- Properties, American Society of Mechanical Engineers,
Academic Press, New York, 1962, pp. 271-278.
49. Probstein, Ronald F. "Inviscid Flow in the Stagnation Point Region of Very Blunt-Nosed Bodies at Hypersonic Flight Speeds." WADC TN 56-395, Sept. 1956.
 50. Potter, J. Leith and Bailey, Allan B. "Pressures in the Stagnation Regions of Blunt Bodies in the Viscous-Layer to Merged-Layer Regimes of Rarefied Flow." AEDC-TDR-63-168 (AD 416004), Sept. 1963.
 51. Kemp, Nelson H., Rose, Peter H. and Detra, Ralph W. "Laminar Heat Transfer Around Blunt Bodies in Dissociated Air." Journal of the Aeronautical Sciences, Vol. 26, No. 7, July 1959, pp. 421-430.
 52. Dorrance, William H. Viscous Hypersonic Flow, McGraw-Hill, New York, 1962, pp. 94-100.
 53. Vidal, R. J. and Wittliff, C. E. "Hypersonic Low Density Studies of Blunt and Slender Bodies." Rarefied Gas Dynamics, Vol. II, Edited by J. A. Laurmann, Academic Press, New York, 1963, pp. 212-227.
 54. Hickman, R. S. "The Influence of Shock Wave-Boundary Layer Interaction on Heat Transfer to an Axisymmetric Body." ARL 62-442, October 1962.
 55. Prok, George M. "Effect of Surface Preparation and Gas Flow on Nitrogen Atom Surface Recombination." NASA TN D-1090, Sept. 1961.
 56. Prok, George M. "Nitrogen and Oxygen Atom Recombination at Oxide Surfaces and Effect of a Tesla Discharge on Recombination Heat Transfer." NASA TN D-1567, Jan. 1963.
 57. Myerson, A. L. "Interim Report on Transient Heat-Transfer Measurements of Catalytic Recombination in a Step-Function Flow of Atomic Oxygen." Cornell Aeronautical Laboratory Report No. AF-1412-A-2, August 1962.
 58. Rosner, Daniel E. "Analysis of Air Arc-Tunnel Heat-Transfer Data." AIAA Journal, Vol. 2, No. 5, May 1964, pp. 945-948.
 59. Rosner, Daniel E. "Boundary Conditions for the Flow of a Multi-component Gas." Jet Propulsion, Vol. 28, No. 8, Aug. 1958, pp. 555-556.
 60. Ammann, H. H. "Heterogeneous Recombination and Heat Transfer with Dissociated Nitrogen." Ph. D. Dissertation, Purdue University, January 1964.

61. Hoshizaki, H., Neice, S., and Chan, K. K. "Stagnation Point Heat Transfer Rates at Low Reynolds Numbers." IAS Paper No. 60-68, June 1960.
62. Ferri, A., Zakkay, V. and Ting, L. "Blunt Body Heat Transfer at Hypersonic Speed and Low Reynolds Numbers." PIBAL Report No. 611, ARL Technical Note 60-140, June 1960.
63. Ferri, A. and Zakkay, V. "Measurements of Stagnation Point Heat Transfer at Low Reynolds Numbers." PIBAL 644, ARL 38, April 1961.
64. Varwig, Robert L. "Stagnation Point Heat Transfer Measurements in Hypersonic Low Reynolds Number Flows." Aerospace Corp. Rept. No. TDR-930 (2230-11) TN-2, June 1962.
65. Bloxsom, D. E. and Rhodes, B. V. "Experimental Effect of Bluntness and Gas Rarefaction on Drag Coefficients and Stagnation Heat Transfer on Axisymmetric Shapes in Hypersonic Flow." Journal of the Aerospace Sciences, Vol. 29, No. 12, Dec. 1962, pp. 1429-1432.
66. Potter, J. L. and Miller, J. T. "Total Heating Load on Blunt Axisymmetric Bodies in Low-Density Flow." AIAA Journal, Vol. 1, No. 2, February 1963, pp. 480-481.

A E D C - T R - 6 5 - 1 2 7



A E D C
1676-U

Fig. 1 Photograph of Gas Dynamic Wind Tunnel, Hypersonic (L) from the Operator's Side

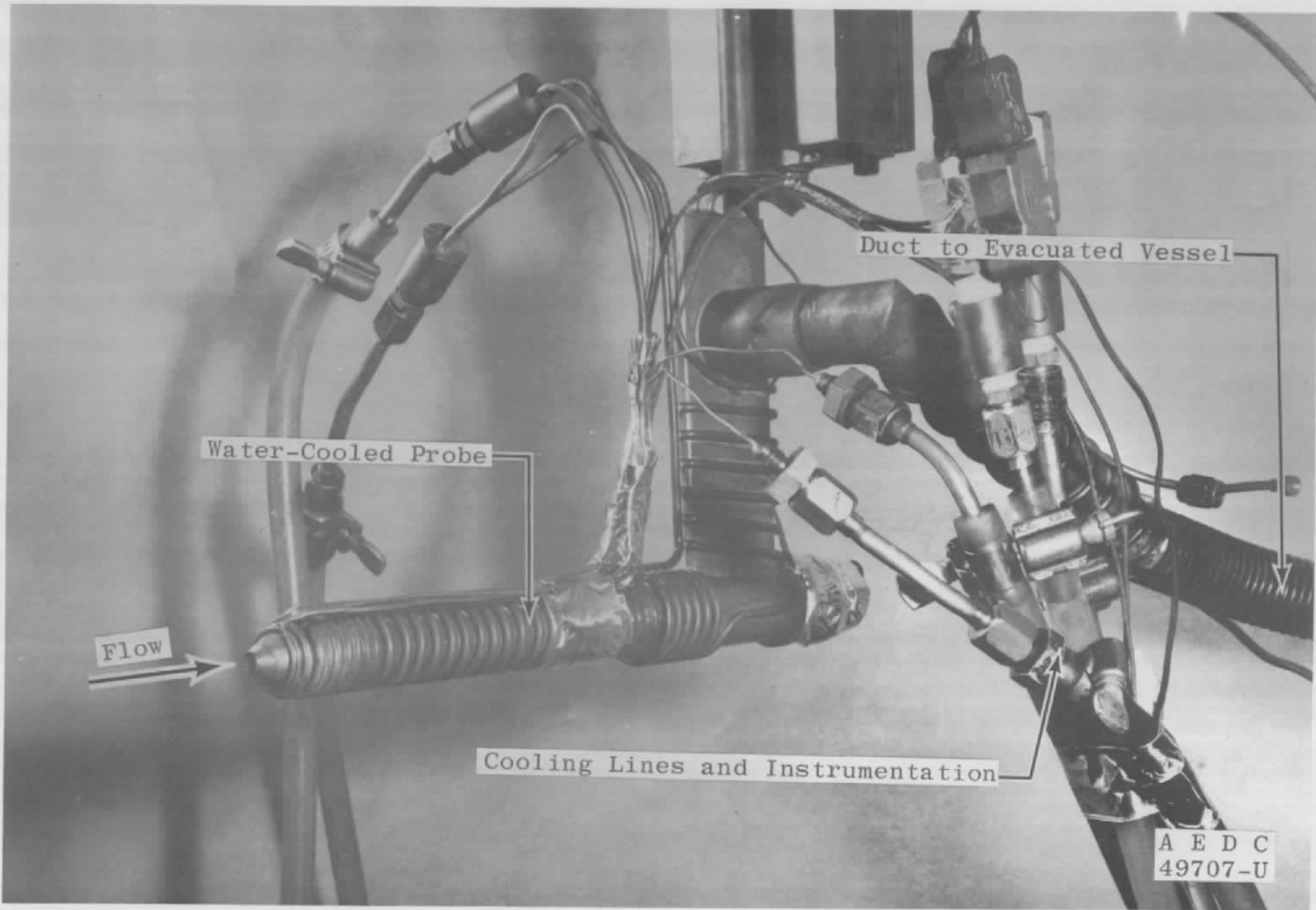


Fig. 2 Total-Enthalpy and Mass-Flow Probe Installed in Tunnel

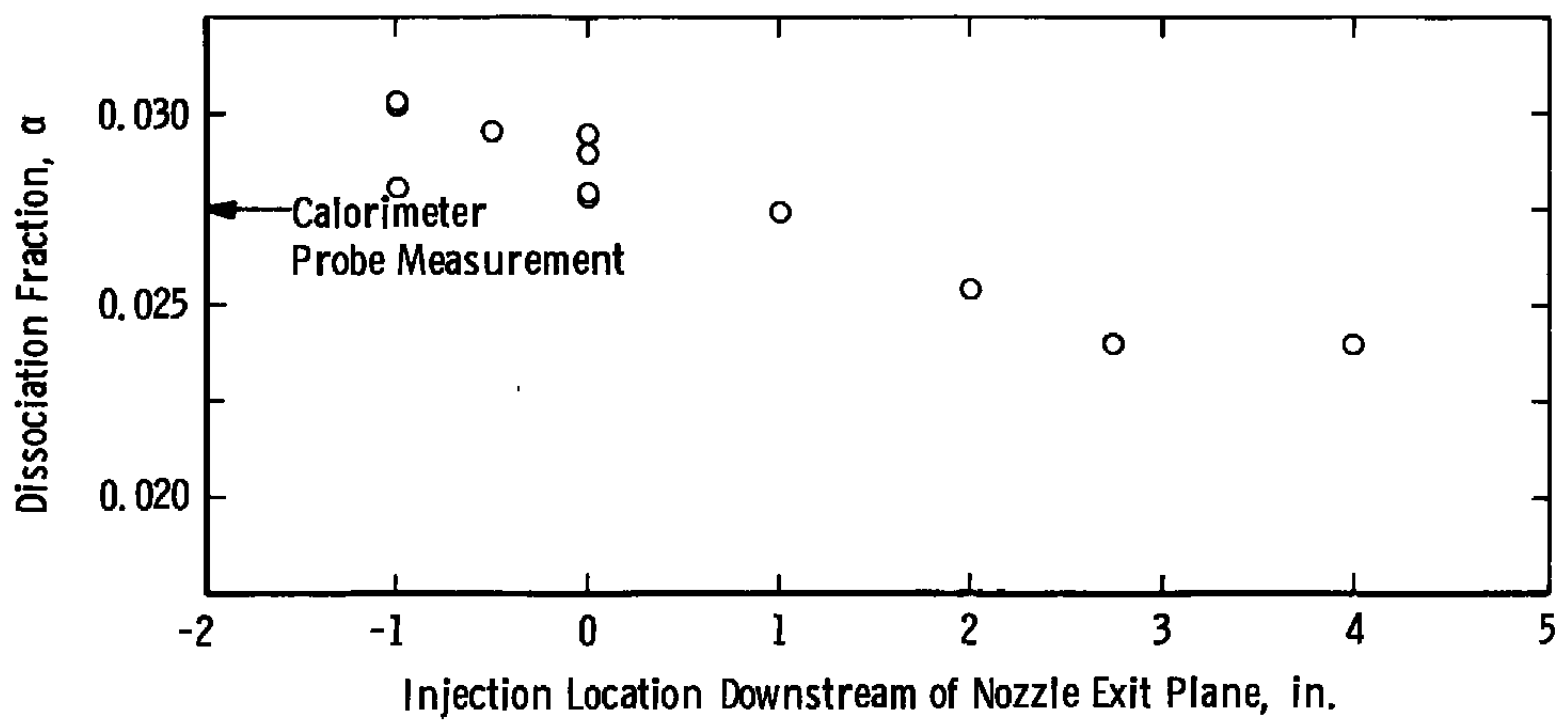


Fig. 3 Dissociation Fraction Measured by Nitric Oxide Titration

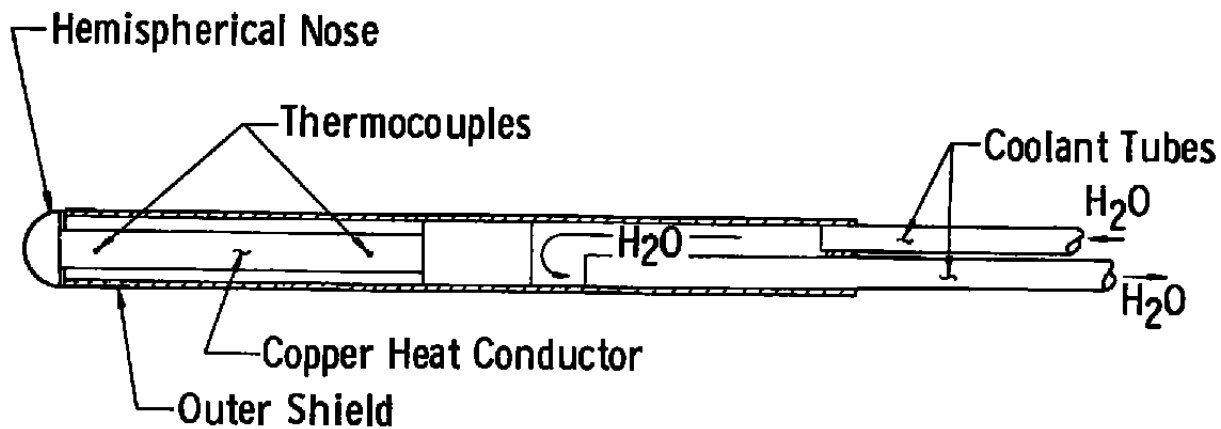


Fig. 4 Water-Cooled Heat Transfer Probe

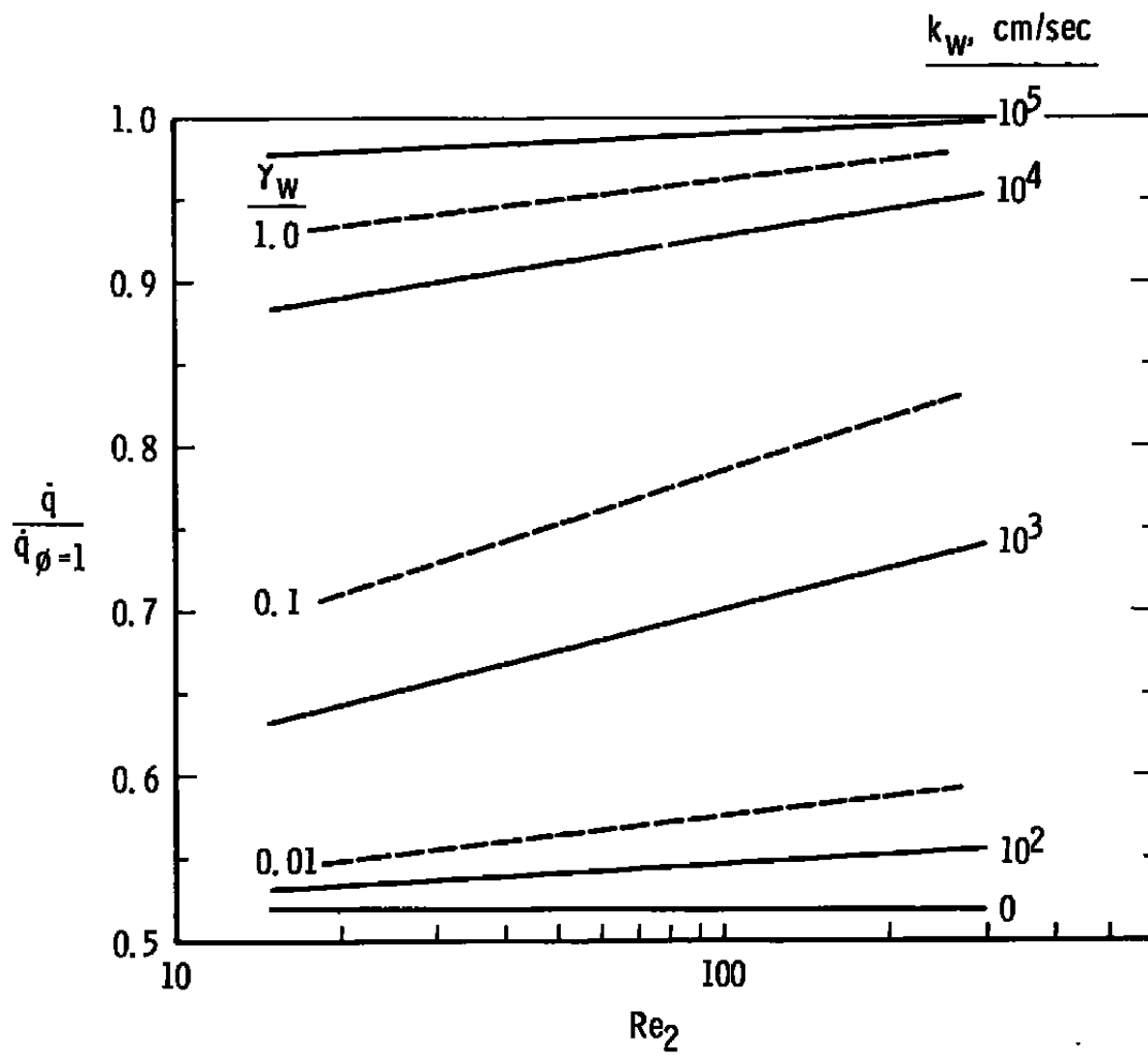


Fig. 5 Effect of Finite Surface Catalytic Properties

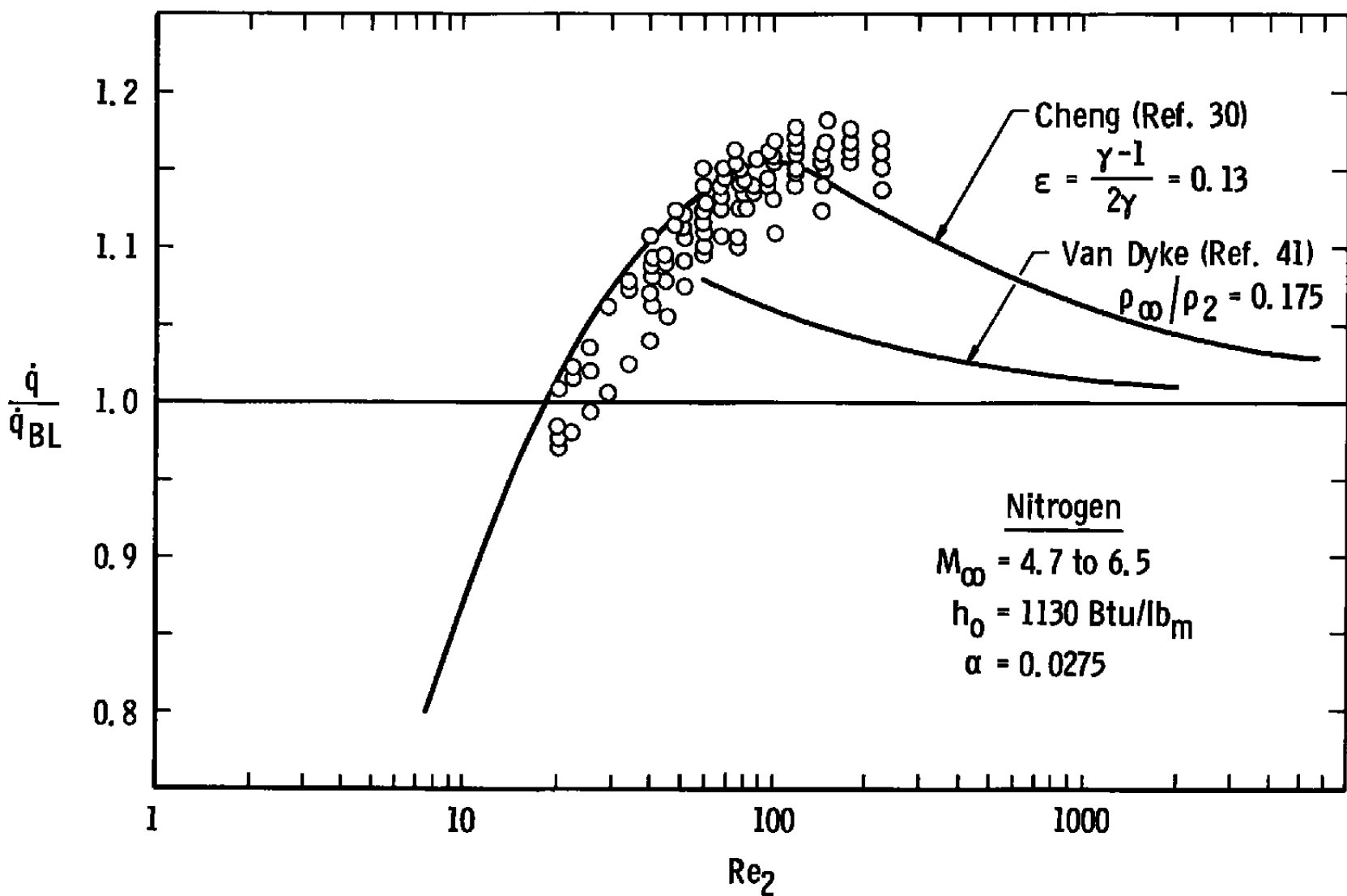


Fig. 6 Heat Transfer to Copper Hemispheres for $\phi = 1$

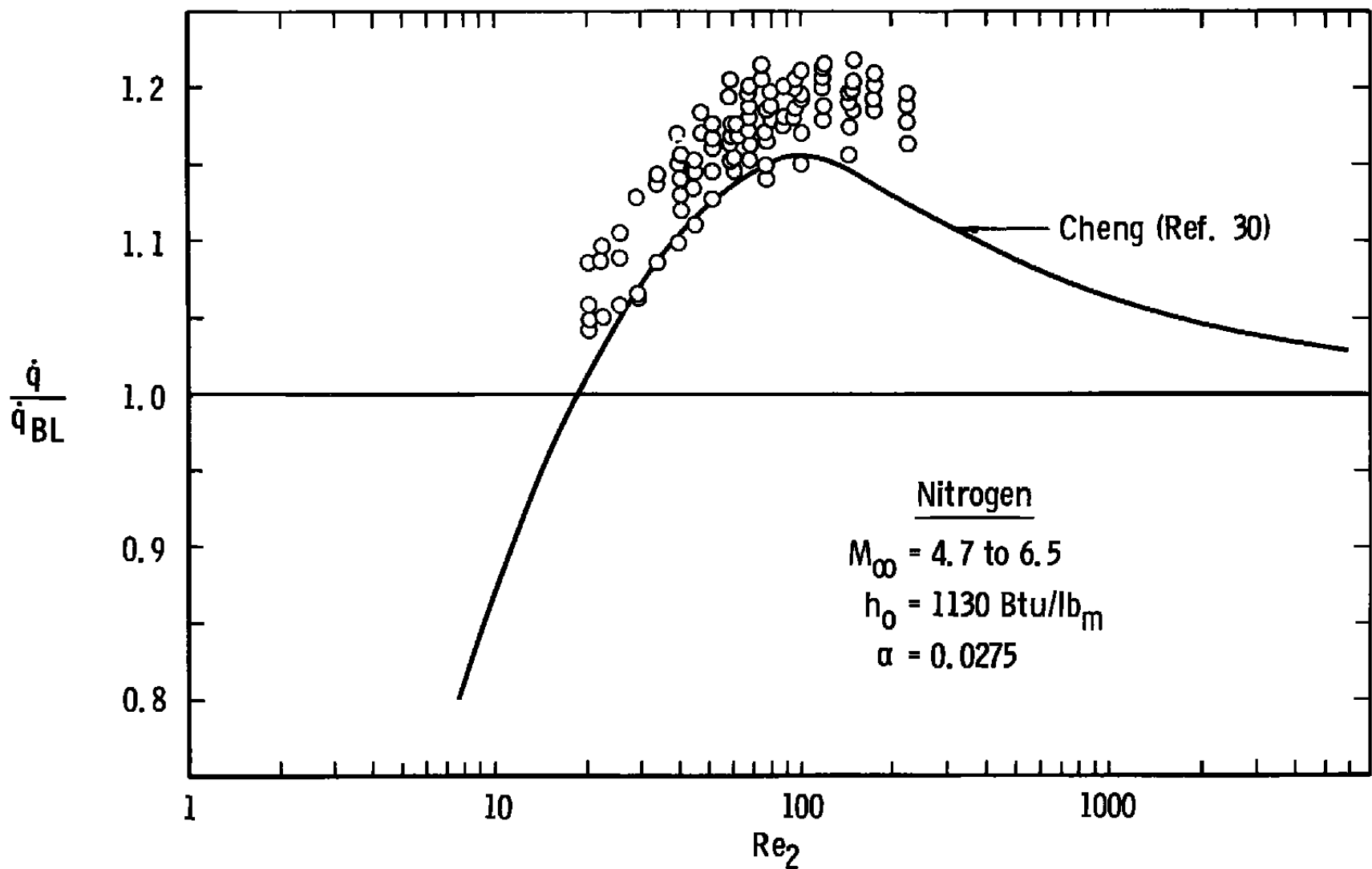


Fig. 7 Heat Transfer to Copper Hemispheres for $\gamma_w = 1$

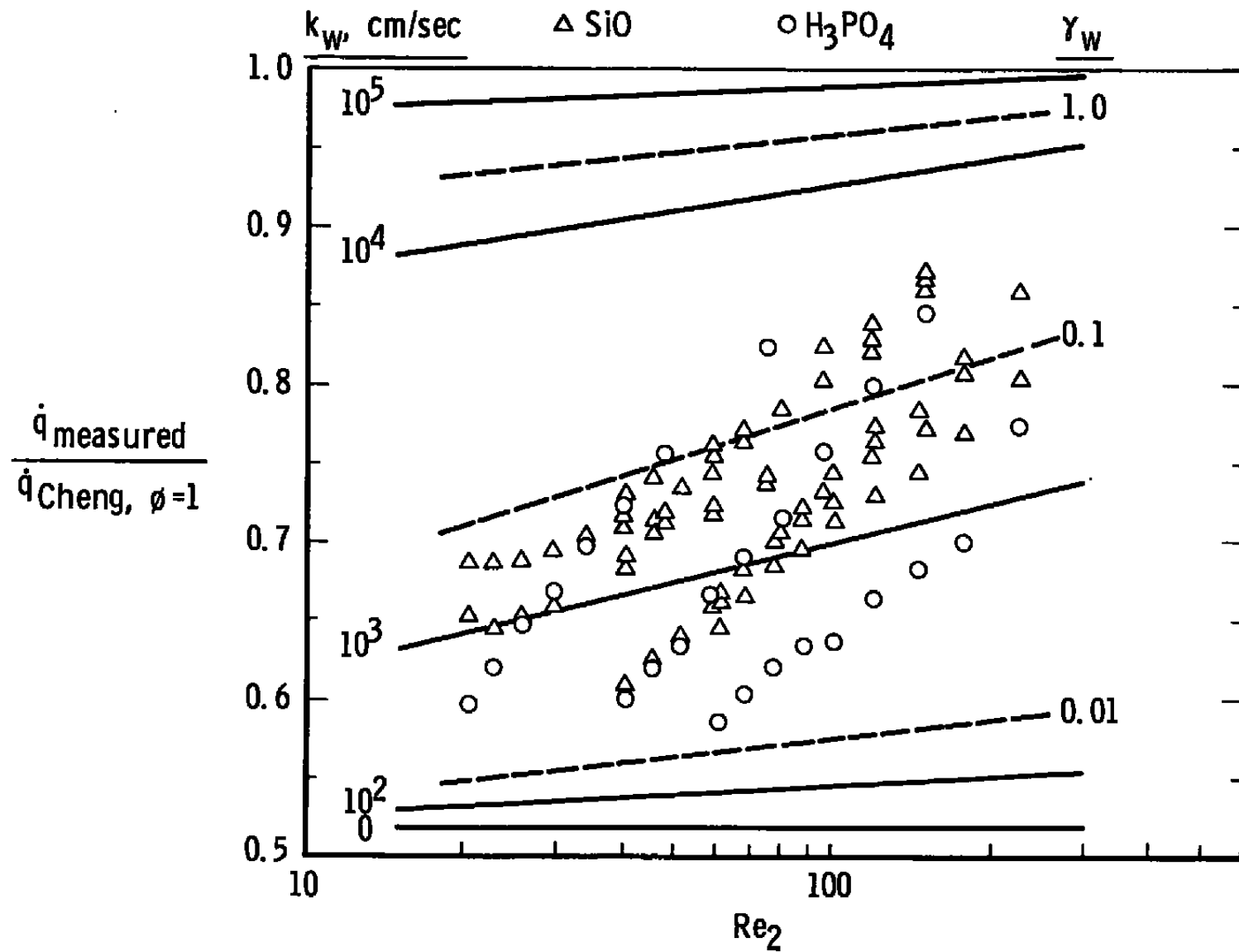


Fig. 8 Heat Transfer to Hemispheres with Coated Surfaces

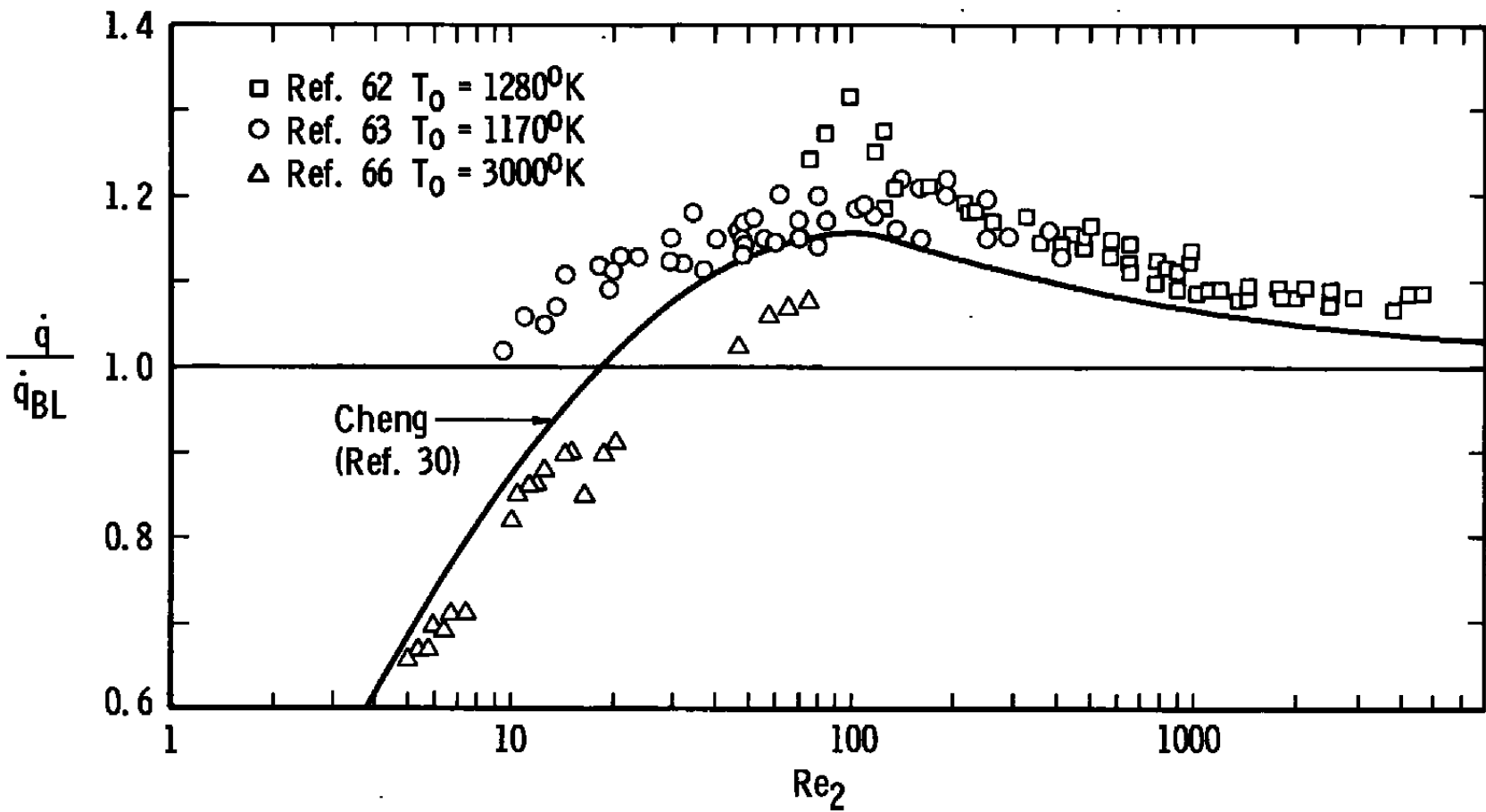


Fig. 9 Some Previous Stagnation Heat Transfer Measurements at Low Reynolds Numbers

TABLE I
TUNNEL FLOW CONDITIONS

Location Downstream of Nozzle Exit Plane, in. ²	0	1	2	3	4
M_∞	4.73	5.28	5.75	6.13	6.48
U_∞ ft/sec	5376	5474	5536	5580	5618
ρ_∞ lb _m /ft ³ x 10 ⁴	0.4703	0.2965	0.2059	0.1557	0.1217
Re_2 /in.	599	385	270	206	162

UNCLASSIFIED

Security Classification

DOCUMENT CONTROL DATA - R&D

(Security classification of title, body of abstract and indexing annotation must be entered when the overall report is classified)

1 ORIGINATING ACTIVITY (Corporate author) Arnold Engineering Development Center ARO, Inc., Operating Contractor Arnold Air Force Station, Tennessee		2a REPORT SECURITY CLASSIFICATION UNCLASSIFIED
		2b GROUP N/A
3 REPORT TITLE EXPERIMENTAL HEAT TRANSFER TO HEMISPHERES IN NONEQUILIBRIUM DISSOCIATED HYPERSONIC FLOW WITH SURFACE CATALYSIS AND SECOND- ORDER EFFECTS		
4 DESCRIPTIVE NOTES (Type of report and inclusive dates) N/A		
5. AUTHOR(S) (Last name, first name, initial) Carden, William H., ARO, Inc.		
6. REPORT DATE July 1965	7a. TOTAL NO. OF PAGES 46	7b. NO. OF REFS 66
8a. CONTRACT OR GRANT NO. AF 40(600)-1000	8a. ORIGINATOR'S REPORT NUMBER(S)	
b. PROJECT NO. 8950	AEDC-TR-65-127	
c. Program Element 62405334	9b. OTHER REPORT NO(S) (Any other numbers that may be assigned this report) N/A	
d.		
10. AVAILABILITY/LIMITATION NOTICES Qualified users may obtain copies of this report from DDC.		
11. SUPPLEMENTARY NOTES N/A	12. SPONSORING MILITARY ACTIVITY Arnold Engineering Development Center Air Force Systems Command Arnold Air Force Station, Tennessee	
13 ABSTRACT An experimental investigation of heat transfer to hemispheres with both catalytic and noncatalytic surfaces in nonequilibrium dissociated hypersonic nitrogen flow has been conducted. The wind tunnel flow conditions provided low Reynolds numbers, allowing the assumption of completely frozen shock and boundary layers while introducing the influences of second-order boundary layer effects such as vorticity interaction. The results for copper surfaces, when correlated using the stagnation point heat transfer equation of Rosner together with Lees' heat transfer distribution, are in good agreement with the second-order theory of Cheng under the assumption of complete surface recombination of atoms. Reductions in heat transfer rate up to 30 percent were obtained with the use of noncatalytic coatings applied to the probes.		

UNCLASSIFIED

Security Classification

14 KEY WORDS	LINK A		LINK B		LINK C	
	ROLE	WT	ROLE	WT	ROLE	WT
heat transfer hemispheres hypersonic flow nonequilibrium. surface catalysis second-order effects noncatalytic coatings						

INSTRUCTIONS

1. ORIGINATING ACTIVITY: Enter the name and address of the contractor, subcontractor, grantee, Department of Defense activity or other organization (corporate author) issuing the report.

2a. REPORT SECURITY CLASSIFICATION: Enter the overall security classification of the report. Indicate whether "Restricted Data" is included. Marking is to be in accordance with appropriate security regulations.

2b. GROUP: Automatic downgrading is specified in DoD Directive 5200.10 and Armed Forces Industrial Manual. Enter the group number. Also, when applicable, show that optional markings have been used for Group 3 and Group 4 as authorized.

3. REPORT TITLE: Enter the complete report title in all capital letters. Titles in all cases should be unclassified. If a meaningful title cannot be selected without classification, show title classification in all capitals in parenthesis immediately following the title.

4. DESCRIPTIVE NOTES: If appropriate, enter the type of report, e.g., interim, progress, summary, annual, or final. Give the inclusive dates when a specific reporting period is covered.

5. AUTHOR(S): Enter the name(s) of author(s) as shown on or in the report. Enter last name, first name, middle initial. If military, show rank and branch of service. The name of the principal author is an absolute minimum requirement.

6. REPORT DATE: Enter the date of the report as day, month, year, or month, year. If more than one date appears on the report, use date of publication.

7a. TOTAL NUMBER OF PAGES: The total page count should follow normal pagination procedures, i.e., enter the number of pages containing information.

7b. NUMBER OF REFERENCES: Enter the total number of references cited in the report.

8a. CONTRACT OR GRANT NUMBER: If appropriate, enter the applicable number of the contract or grant under which the report was written.

8b, 8c, & 8d. PROJECT NUMBER: Enter the appropriate military department identification, such as project number, subproject number, system numbers, task number, etc.

9a. ORIGINATOR'S REPORT NUMBER(S): Enter the official report number by which the document will be identified and controlled by the originating activity. This number must be unique to this report.

9b. OTHER REPORT NUMBER(S): If the report has been assigned any other report numbers (either by the originator or by the sponsor), also enter this number(s).

10. AVAILABILITY/LIMITATION NOTICES: Enter any limitations on further dissemination of the report, other than those

imposed by security classification, using standard statements such as:

- (1) "Qualified requesters may obtain copies of this report from DDC."
- (2) "Foreign announcement and dissemination of this report by DDC is not authorized."
- (3) "U. S. Government agencies may obtain copies of this report directly from DDC. Other qualified DDC users shall request through _____."
- (4) "U. S. military agencies may obtain copies of this report directly from DDC. Other qualified users shall request through _____."
- (5) "All distribution of this report is controlled. Qualified DDC users shall request through _____."

If the report has been furnished to the Office of Technical Services, Department of Commerce, for sale to the public, indicate this fact and enter the price, if known.

11. SUPPLEMENTARY NOTES: Use for additional explanatory notes.

12. SPONSORING MILITARY ACTIVITY: Enter the name of the departmental project office or laboratory sponsoring (paying for) the research and development. Include address.

13. ABSTRACT: Enter an abstract giving a brief and factual summary of the document indicative of the report, even though it may also appear elsewhere in the body of the technical report. If additional space is required, a continuation sheet shall be attached.

It is highly desirable that the abstract of classified reports be unclassified. Each paragraph of the abstract shall end with an indication of the military security classification of the information in the paragraph, represented as (TS), (S), (C), or (U).

There is no limitation on the length of the abstract. However, the suggested length is from 150 to 225 words.

14. KEY WORDS: Key words are technically meaningful terms or short phrases that characterize a report and may be used as index entries for cataloging the report. Key words must be selected so that no security classification is required. Identifiers, such as equipment model designation, trade name, military project code name, geographic location, may be used as key words but will be followed by an indication of technical context. The assignment of links, rules, and weights is optional.

UNCLASSIFIED

Security Classification